Articles

Orientational and Stereochemical Preferences in [Hydridotris(3,5-dimethyl-1-pyrazolyl)borato](CO)$_2$W(η^3-allyl) Complexes

David S. Frohnapfel, Peter S. White, and Joseph L. Templeton*

W. R. Kenan, Jr. Laboratory, Department of Chemistry, University of North Carolina, Chapel Hill, North Carolina 27514

Heinz Rüegger and Paul S. Pregosin*

Laboratorium für Anorganische Chemie, Eidgenössische Technische Hochschule, CH-8092 Zürich, Switzerland

Received February 3, 1997[⊗]

Irradiation of Tp′(CO)$_3$WH in the presence of alkynes or unconjugated dienes generates η^3-allyl complexes, Tp′(CO)$_2$W(η^3-CHRCHCHR′). A kinetic preference for *anti*-alkyl substitution due to η^2-vinyl intermediates exists for the reactions with terminal alkyne substrates. The monoalkyl-substituted allyl complexes are configurationally stable on the NMR time scale but show a thermodynamic preference for *syn*-substitution upon heating in solution. Separate crystal structures of the *syn* and *anti* isomers of the 1-methylallyl complex, Tp′(CO)$_2$W(η^3-CH$_2$CHCHCH$_3$), have revealed isomers which differ by approximately 90° in allyl orientation (θ). The term *meso* is introduced to emphasize the orthogonal relationship between the *anti* (θ = 30°, *exo*) and the *syn* (θ = 120°, *meso*) isomers. The change in orientation of the allyl is accompanied by a change in the OC−W−CO angle from acute to obtuse in order to maximize donation from the π-nonbonding orbital of the allyl into the dπ metal orbitals. EHMO (extended Hückel molecular orbital) calculations on a model complex [H$_3$W(CO)$_2$(η^3-C$_3$H$_5$)]$^{2-}$ show electronic minima at θ = 30° and 115° corresponding to the two orientations.

Introduction

Group VI transition metal η^3-allyl complexes containing tris(pyrazolyl)borate ligands (Tp = hydridotris(1-pyrazolyl)borate; Tp′ = hydridotris(3,5-dimethyl-1-pyrazolyl)borate) were first reported in the late 1960s by Trofimenko.[1,2] Analogous cyclopentadienyl (Cp) complexes have been thoroughly studied,[3−10] and Cp-based η^3-allyl complexes have been used in stoichiometric transformations leading to organic products.[11−19] Less information is available regarding stereochemical preferences for Tp and Tp′ allyl complexes, but there has been a recent resurgence of interest in the chemistry of tris(pyrazolyl)borate group VI metal allyl complexes.[20−25]

Approaches utilizing nucleophilic attack by a metal species on allyl halides have been used to form Cp(CO)$_2$Mo(η^3-allyl) and Tp(CO)$_2$Mo(η^3-allyl) complexes.[1,5,6,23,26] Analogous Tp′(CO)$_2$W(η^3-allyl) complexes are more elusive synthetically since the [Tp′(CO)$_3$W]$^-$ anion does not add to allyl halides.[1]

[⊗] Abstract published in *Advance ACS Abstracts,* July 15, 1997.

(1) Trofimenko, S. *J. Am. Chem. Soc.* **1969**, *91*, 588.
(2) Trofimenko, S. *J. Am. Chem. Soc.* **1969**, *91*, 3183.
(3) Davison, A.; Rode, W. C. *Inorg. Chem.* **1967**, *6*, 2124.
(4) Faller, J. W.; Incorvia, M. J. *Inorg. Chem.* **1968**, *7*, 840.
(5) Merour, J. Y.; Charrier, C.; Benaim, J.; Roustan, J. L. *J. Organomet. Chem.* **1972**, *39*, 321.
(6) Faller, J. W.; Chen, C. C.; Mattina, M. J.; Jakubowski, A. *J. Organomet. Chem.* **1973**, *52*, 361.
(7) Huttner, G.; Brintzinger, H. H.; Bell, L. G.; Friedrich, P.; Bejenke, V.; Neugebauer, D. *J. Organomet. Chem.* **1978**, *145*, 329.
(8) Greenhough, T. J.; Legzdins, P.; Martin, D. T.; Trotter, J. *Inorg. Chem.* **1979**, *18*, 3268.
(9) Faller, J. W.; Chodosh, D. F.; Katahira, D. *J. Organomet. Chem.* **1980**, *187*, 227.
(10) Krivykh, V. V.; Gusev, O. V.; Petrovskii, P. V.; Rybinskaya, M. I. *J. Organomet. Chem.* **1989**, *366*, 129.
(11) Faller, J. W.; Linebarrier, D. *Organometallics* **1988**, *7*, 1670.
(12) Faller, J. W.; Lambert, C.; Mazzieri, M. R. *J. Organomet. Chem.* **1990**, *383*, 161.
(13) Pearson, A. J.; Mallik, S.; Mortezaei, R.; Perry, M. W. D.; Shively, R. J.; Youngs, W. J. *J. Am. Chem. Soc.* **1990**, *112*, 8034.
(14) Vong, W.; Peng, S.; Lin, S.; Lin, W.; Liu, R. *J. Am. Chem. Soc.* **1990**, *113*, 573.
(15) Lin, S.; Peng, S.; Liu, R. *J. Chem. Soc., Chem. Commun.* **1992**, 615.
(16) Yang, G.; Su, G.; Liu, R. *Organometallics* **1992**, *11*, 3444.
(17) Faller, J. W.; Nguyen, J. T.; Ellis, W.; Mazzieri, M. R. *Organometallics* **1993**, *12*, 1434.
(18) Yu, R. H.; McCallum, J. S.; Liebeskind, L. S. *Organometallics* **1994**, *13*, 1476.
(19) Lin, S.; Chen, C.; Vong, W.; Liu, R. *Organometallics* **1995**, *14*, 1619.
(20) Feng, S. G.; Templeton, J. L. *Organometallics* **1992**, *11*, 2168.
(21) Pregosin, P. S.; Macchioni, A.; Templeton, J. L.; White, P. S.; Feng, S. G. *Magn. Reson. Chem.* **1994**, *32*, 415.
(22) Joshi, V. S.; Sathe, K. M.; Nandi, M.; Chakrabarti, P.; Sarkar, A. *J. Organomet. Chem.* **1995**, *485*, C1.
(23) Ward, Y. D.; Villanueva, L. A.; Allred, G. D.; Payne, S. C.; Semones, M. A.; Liebeskind, L. S. *Organometallics* **1995**, *14*, 4132.
(24) Villanueva, L. A.; Ward, Y. D.; Lachicotte, R.; Liebeskind, L. S. *Organometallics* **1996**, *15*, 4190.
(25) Ward, Y. D.; Villanueva, L. A.; Allread, G. D.; Liebeskind, L. S. *Organometallics* **1996**, *15*, 4201.
(26) Hayter, R. G. *J. Organomet. Chem.* **1968**, *13*, P1.

S0276-7333(97)00074-5 CCC: $14.00

Chart 1. Isomer Possibilities and Labeling Scheme for Allyl Complexes

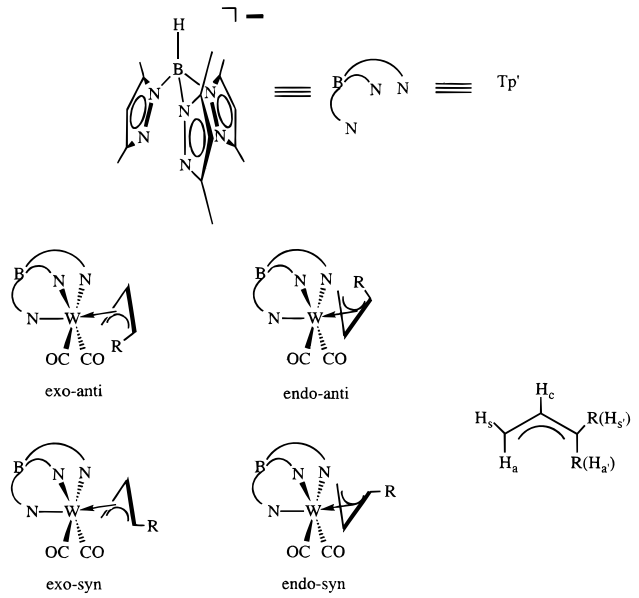

Nucleophilic addition to cationic 4 e⁻ donor alkyne complexes is known to produce η^3-allyl complexes from η^2-vinyl intermediates having β-hydrogens.[20,27,28] Alt and co-workers have reported the generation of η^3-allyl complexes from irradiation of Cp*W(CO)$_3$H (Cp* = pentamethylcyclopentadienyl) in the presence of alkynes.[29] The known photoreactivity of Tp′(CO)$_3$WH suggested that similar routes to Tp′(CO)$_2$W(η^3-allyl) complexes might be practical.[30]

Monosubstituted allyl complexes of the type Tp′(CO)$_2$M(η^3-CH$_2$CHCHR) are normally categorized as one of four isomers corresponding to *endo*/*exo* and *syn*/*anti* combinations. The *endo* ("in") and *exo* ("out") notations refer to the orientation of the allyl fragment relative to the Tp′ ligand (Chart 1). Faller has distinguished *endo* isomers from *exo* isomers for (η^5-indenyl)(CO)$_2$Mo(η^3-allyl) complexes based on the magnetic anisotropy of the indenyl ring.[6] Determination of the *syn* and *anti* configurations for monosubstituted allyl complexes has often been accomplished by consideration of coupling constant values, since coupling between the central proton and *anti* protons tends to be larger ($^3J_{ca} = {}^3J_{ca}' \approx 8-11$ Hz) than coupling between H$_c$ and *syn* protons ($^3J_{cs} = {}^3J_{cs}' \approx 5-8$ Hz). For monosubstituted allyls of the form (η^5-L)(CO)$_2$M(η^3-allyl) (L = C$_5$H$_5$, C$_9$H$_7$; M = Mo, W), *syn* substitution predominates at equilibrium (>95%).[5,6] In contrast, *anti* substitution is preferred for alkyl substituents in allyl complexes containing the tris(1-pyrazolyl)borate ligand (Tp).[23]

We report here the synthesis, through both photochemical and thermal routes, of Tp′(CO)$_2$W(η^3-allyl) complexes. A variable-temperature NMR study of the *syn*-phenylallyl complex is presented. We also document allyl isomers which differ by approximately 90° in allyl rotation, in contrast to the 180° rotation which characterizes *exo*/*endo* isomers in Cp-based allyl complexes. The different orientations adopted by the allyl complexes are accompanied by a significant change (acute vs obtuse) in the OC−W−CO bond angle. Extended Hückel molecular orbital (EHMO) calculations have been performed to clarify the connection between allyl orientation and OC−W−CO bond angle.

Results and Discussion

Synthesis of Tp′(CO)$_2$W(η^3-allyl) Complexes. Both the tungsten parent allyl, Tp′(CO)$_2$W(η^3-C$_3$H$_5$) (**1**), and the 1-methylallyl complex, **2**, were accessible from (EtCN)$_3$W(CO)$_3$ and the appropriate allyl halide by treatment with KTp′ (eq 1). The 1-methylallyltungsten

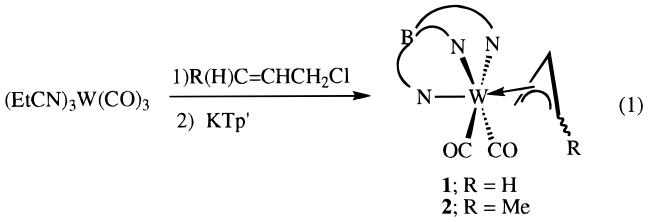

(1)

complex, Tp′(CO)$_2$W(η^3-CH$_2$CHCHMe), exists as two isomers, **2a** and **2s** (**a** = *anti*; **s** = *syn*). The ratio of isomers from the trisnitrile reaction after chromatography was 1:2.3 (**a**:**s**). Isolation of a single isomer (**2a**) from the reaction of a cationic 2-butyne complex with a hydride source was reported earlier.[20] Reflux of a sample of **2a** for 3 h in toluene induced conversion of **2a** to **2s** to produce a static isomer ratio of 1:1.7 (**a**:**s**).

Complex **2** was obtained in a **2a**:**2s** ratio of 19:1 through irradiation of a THF solution containing Tp′(CO)$_3$WH and 2-butyne (eq 2). Spectroscopic evidence

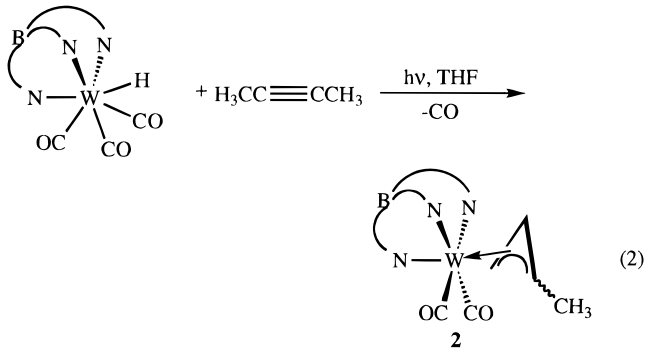

(2)

for an η^2-vinyl intermediate, presumably Tp′(CO)$_2$W(η^2-C(Me)=CHMe) as reported for the alkyne reduction route,[20] was also obtained by the photochemical route. Green has described a reaction mechanism to account for η^3-allyl formation from η^2-vinyl precursors.[27,28] This route exhibits a kinetic preference for *anti* stereochemistry.

The 1-ethylallyl (**3**) and the 1-propylallyl (**4**) complexes were prepared in moderate yields through photolysis of Tp′(CO)$_3$WH with unconjugated dienes (eq 3). Although mechanistic studies have not been carried out, the reaction presumably proceeds by the photolabilization of carbon monoxide,[31,32] binding of a diene terminus,

(27) Allen, S. R.; Baker, P. K.; Barnes, S. G.; Bottrill, M.; Green, M. G.; Orpen, A. G.; Williams, I. D.; Welch, A. *J. Chem. Soc., Dalton Trans.* **1983**, 927.
(28) Green, M. *J. Organomet. Chem.* **1986**, *300*, 93.
(29) Alt, H. G.; Englehardt, H. E.; Wrackmeyer, B.; Rogers, R. D. *J. Organomet. Chem.* **1989**, *379*, 289.
(30) Feng, S. G.; White, P. S.; Templeton, J. L. *J. Am. Chem. Soc.* **1994**, *116*, 8613.
(31) Kazlauskas, R. J.; Wrighton, M. S. *J. Am. Chem. Soc.* **1982**, *104*, 6005.
(32) Virrels, I. G.; George, M. W.; Johnson, F. P. A.; Turner, J. J.; Westwell, J. R. *Organometallics* **1995**, *14*, 5203.

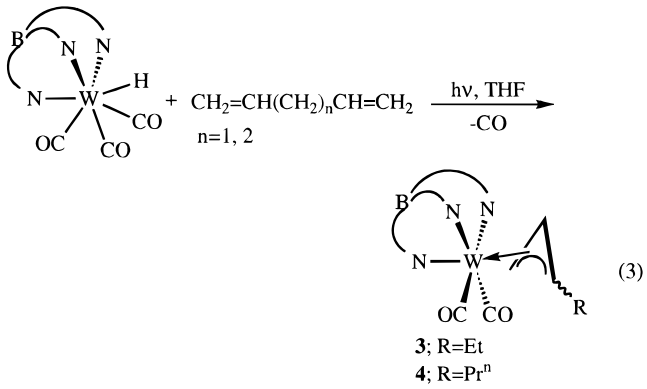

(3)

insertion to form a metal alkyl, and isomerization via β-hydrogen migrations until the thermodynamic product is formed (Scheme 1). No intermediates have been detected. A slight kinetic preference for the **a** isomer was noted (ca. 3:1, **a**:**s**) with the exact ratio depending on the photolysis time. Thermodynamic isomer ratios of 1:1.2 (**a**:**s**) were obtained following an hour reflux period in toluene.

The putative η^2-vinyl complexes possessing β-hydrogens along the path to η^3-allyls led us to consider using η^2-vinyl complexes as starting materials.[33] Efficient conversion of the η^2-vinyl complexes to the η^3-isomers was accomplished in toluene at elevated temperatures (eq 4).

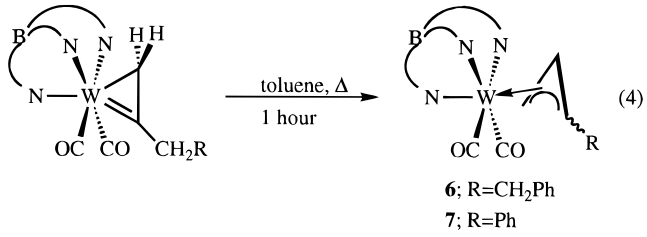

(4)

Two isomers of the 1-benzylallyl complex, **5a** and **5s**, were obtained in an isomer ratio of 1:1.9 (**a**:**s**), and the isomer ratio remained unchanged over time. The *syn*-1-phenylallyl complex, **6**, previously prepared by hydride addition to a phenylacetylene complex,[20] was synthesized here by irradiating $Tp'(CO)_3WH$ in the presence of 3-phenyl-1-propyne. An η^2-vinyl intermediate, presumably $Tp'(CO)_2W(\eta^2\text{-}C(CH_2Ph)=CH_2)$, was observed in the IR spectrum of the reaction mixture during irradiation. Although only one isomer for **6** is evident in the room-temperature ^1H NMR spectrum, two isomers were observed by low-temperature NMR (*vide infra*).

Prolonged photolysis of $Tp'(CO)_3WH$ in the presence of 1-phenyl-1-butyne initially produced a mixture of η^2-vinyl and η^3-allyl products. Subsequent heating in toluene for 1 h effected complete conversion to the disubstituted η^3-allyl product. Two isomers, **7a** and **7s**, were obtained in an isomer ratio of 1:1.3 (**a**:**s**). In an attempt to synthesize the 1,3-dimethyl-substituted allyl complex, $Tp'(CO)_3WH$ was irradiated in the presence of 2-pentyne. Only the 1-propylallyl complex, **4**, was isolated from the reaction. The photolysis of $Tp'(CO)_3WH$ with 3-hexyne produced the dialkyl-substituted 1-ethyl-3-methylallyl complex (**8**) in good yield.

(33) Frohnapfel, D. S.; White, P. S.; Templeton, J. L. Unpublished results. The synthesis, characterization, and reactivity of η^2-vinyl complexes will be the subject of a future publication.

Scheme 1

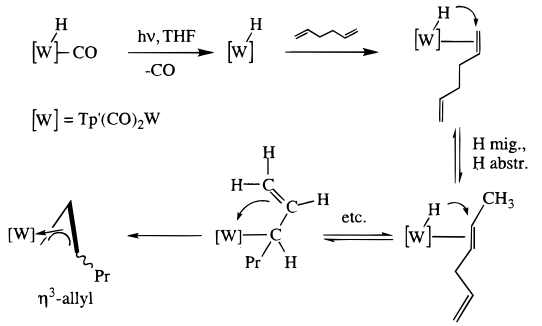

Periodic monitoring of the reaction via IR spectroscopy indicated an η^2-vinyl intermediate. Complex **8** is fluxional in solution on the NMR time scale. The presence of two isomers for **8** was substantiated by low-temperature NMR.

Infrared Spectra of $Tp'(CO)_2M(\eta^3\text{-allyl})$ Complexes. The tungsten monosubstituted allyl complexes show characteristic metal dicarbonyl infrared absorption patterns near 1920 and 1820 cm^{-1}; the frequencies for the molybdenum complexes are slightly higher than those of their tungsten analogs. The carbonyl frequencies for the 1-phenyl-3-methyl complex, **7**, averaged about 15 cm^{-1} lower in energy than those of the monosubstituted complexes.

Repetitive alumina chromatography with 9:1 hexanes:CH_2Cl_2 cleanly separated the two isomers for the 1-methylallyl complex, **2**. Partial separation (>95%) of the corresponding molybdenum complex, **10**, was acheived by this route. This method of separation failed for the more soluble ethyl and propyl complexes and led to significant decomposition of the benzyl complex. The CO stretching frequencies for **2a** averaged about 8 cm^{-1} higher than those of **2s**. This difference in energy is similar to that seen for *endo* and *exo* isomers in the $Cp(CO)_2M(\eta^3\text{-allyl})$ (M = Mo, W) systems.[6]

Clean samples of **2a** and **2s** exhibit a reversal in the relative intensities of the two CO stretching absorptions. In the solid state, the calculated OC−W−CO angle for **2a** was 86° whereas the corresponding angle for **2s** was calculated to be 105°. These calculations are not expected to be precise, but qualitative conclusions, i.e., acute or obtuse, should be valid.[34]

Characterization of the Orientational and Stereochemical Isomers of $Tp'(CO)_2W(\eta^3\text{-}CH_2CHCHCH_3)$. As shown in Table 1, a remarkable consistency was evident in the ^1H NMR spectra of the monosubstituted tungsten allyl complexes (**2**−**5**). Each of the alkyl-substituted complexes exists as two isomers differing in the orientation and stereochemistry (*syn* vs *anti*) of the allyl fragment. Note that the stereochemistry of the allyl moieties cannot be unambiguously assigned on the basis of $^3J_{HH}$ coupling constant values. An earlier 2-D NOESY NMR analysis of **2a**[21] had shown an *anti*-methyl stereochemistry for this isomer, and by extension, an *anti* configuration is proposed for the remaining **a** isomers. A similar NMR study of **2s** proved to be equally informative.

Figure 1 shows relevant sections of the 2-D $^1H\{^{11}B\}$ NOESY (nuclear Overhauser effect spectrometry) spectrum for a mixture of **2a** and **2s**. The cross peaks

(34) Burdett, J. K. *Inorg. Chem.* **1981**, *20*, 2607.

Table 1. ^{1}H NMR Data for Tp′(CO)$_2$M(η^3-CH$_2$CHCHR) (R = CH$_2$R′) Complexes

	M	R	R′	H$_a$	H$_a$′	H$_c$	H$_s$	H$_s$′	−*H*CHR′	−HC*H*R′
2a	W	H		1.97, $^3J_{ac}$ = 9.1		3.17	3.36, $^3J_{sc}$ = 6.5			
2s	W	*anti*-Me	H	2.70		3.28	3.28	4.14	1.61, $^3J_{Mes'}$ = 6.4 2.54, $^3J_{Mea'}$ = 6	
3a	W	*syn*-Me	H	1.57, $^3J_{ac}$ = 8	2.69, $^3J_{a'c}$ = 8	4.97	1.96, $^3J_{sc}$ = 6			
3s	W	*anti*-Et	Me	2.61, $^3J_{ac}$ = 10, $^2J_{as}$ = 2		3.23	3.28, $^3J_{sc}$ = 7, $^4J_{s's}$ = 2	4.15, $^3J_{s'c}$ = 7, $^3J_{HHs'}$ = 11	2.38, $^2J_{HH}$ = 14.4, $^3J_{MeH}$ = 7.4, $^3J_{s'H}$ = 3.6	0.72, $^3J_{s'H}$ = 11
4a	W	*syn*-Et	Me	1.60, $^3J_{ac}$ = 8	2.79−2.72 (m)	5.05, $^3J_{a'c}$ = 6	1.99, $^3J_{sc}$ = 6		2.7−2.6 (m), $^2J_{HH}$ = 13.6, $^3J_{s'H}$ = 3.2	2.58−2.51 (m)
4s	W	*anti*-Pr	Et	2.60, $^3J_{ac}$ = 10		3.21	3.30, $^3J_{sc}$= 7.3, $^4J_{s's}$ = 2, $^2J_{as}$ = 2	4.15, $^3J_{HHs'}$ = 11, $^3J_{s'c}$ = 7.3, $^3J_{s'H}$ = 3, $^4J_{ss'}$ = 2	2.42−2.36 (m)	0.71, $^2J_{HH}$ = 14, $^3J_{s'H}$ = 11, $^3J_{HH}$ = 8.8, $^3J_{HH}$ = 6.2
5a	W	*syn*-Pr	Et	1.61, $^3J_{ac}$ = 8	2.8−2.7 (m)	5.06, $^3J_{a'c}$ = 6	1.98, $^3J_{sc}$ = 6		2.7−2.6 (m)	not located
5s	W	*anti*-Bz	Ph	2.72, $^3J_{ac}$ = 10.2, $^2J_{sa}$ = 1.4		3.13	3.36, $^3J_{sc}$ = 7.2, $^4J_{s's}$ = 1.6	4.31, $^3J_{s'c}$ = 7.4, $^3J_{s'H}$ = 11	3.96, $^2J_{HH}$ = 14.4, $^3J_{s'H}$ = 3.2	1.95−1.93 (m) (obscured)
9	W	*syn*-Bz	Ph	1.58, $^3J_{ac}$ = 8	3.00, $^3J_{a'c}$ = 6	5.23	1.93, $^3J_{sc}$ = 6		3.96, $^2J_{HH}$ = 14.4, $^3J_{a'H}$ = 3.2	3.84, $^3J_{a'H}$ = 10
10a	Mo	H		1.90, $^3J_{ac}$ = 10		4.26	3.64, $^3J_{s'c}$ = 6.7			
10s	Mo	*anti*-Me	H	2.97, $^3J_{ac}$ = 11		4.12	3.50, $^3J_{sc}$ = 7.4, $^4J_{s's}$ = 1.2	4.59, $^3J_{s'c}$ = 7.6, $^3J_{s'Me}$ = 6.8	1.28, $^3J_{s'Me}$ = 6.8	
	Mo	*syn*-Me	H	1.98, $^3J_{ac}$ = 10	2.68 (m)	5.06, $^3J_{a'c}$ = 6.8	2.68, $^3J_{sc}$ = 6.4		2.20, $^3J_{a'Me}$ = 6.4	

[a] Spectra recorded at 400 MHz in C_6D_6. Chemical shifts given in ppm; coupling values given in Hz. Redundant coupling information is presented only once in the table.

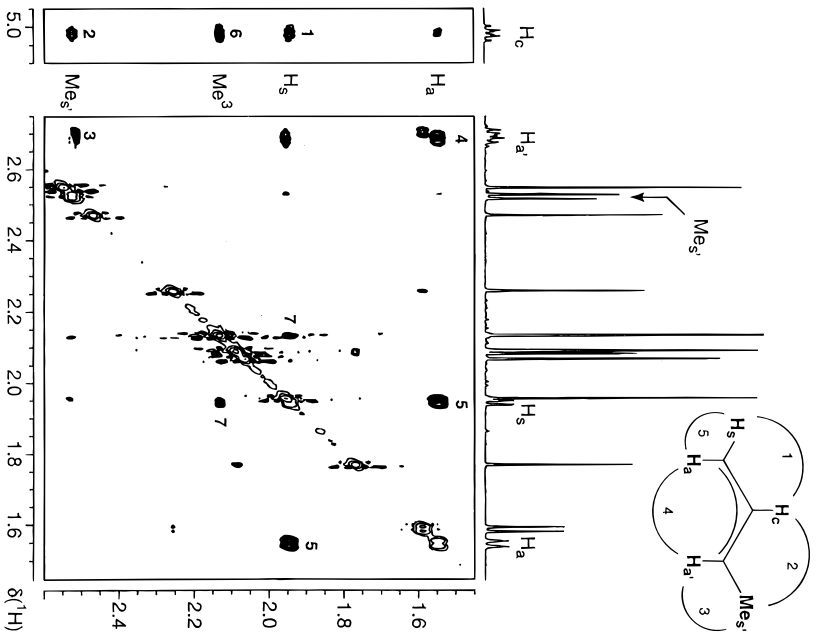

Figure 1. Sections of the 2-D ^{1}H{^{11}B} NOESY spectrum (C_6D_6, room temperature, 500 MHz) for a mixture of **2a** and **2s** showing the relevant cross peaks defining (a) the *syn* stereochemistry of the η^3-1-methylallyl in **2s** (peaks 1−5) and (b) the *meso* orientation of this moiety in the complex (peaks 6 and 7).

numbered 1−5 arise from specific NOEs describing a path around the η^3-1-methylallyl moiety in **2s**. In particular, it is obvious that the methyl group is *syn* to the central proton (H$_c$), based on the NOE contact to H$_c$. It is important to remember that the observed $^3J_{HH}$ allyl coupling constant values for this isomer are not diagnostic and may even be misleading, whereas the NOE spectroscopy provides an unambiguous result.

It is conceivable that dynamic processes, with kinetics on the same time scale as NOE build up, could mask relevant NOE information through mixing of the two incoherent paths for magnetization exchange. Under such conditions, admittedly rare, an alternative structural approach involves the heteronuclear coupling constants $^2J_{WH}$ which are expected to be larger to the central and the *anti*-protons than to the corresponding *syn*-protons. Figure 2 shows a 2-D ^{183}W−^{1}H HMQC (heteronuclear multiple-quantum coherence) spectrum containing these $^2J_{WH}$ data. Note that the amplitude of the cross peaks is proportional to the appropriate scalar heteronuclear coupling. Specifically, one should note the strong cross peak to the *anti*-methyl group in **2a**, whereas the allyl methyl group is "silent" in the *syn*-isomer, **2s**.

Having established the stereochemistry of the allyl fragments in **2a** and **2s**, we turn briefly to the discussion of the solution structure of **2s** (that of **2a** has previously been established[21]). There are strong NOE cross peaks (6 and 7 in Figure 1) for the H$_c$ and H$_s$ protons to the 3-Me group of a *cis*-positioned pyrazole group. To rationalize these specific short contacts, we propose a

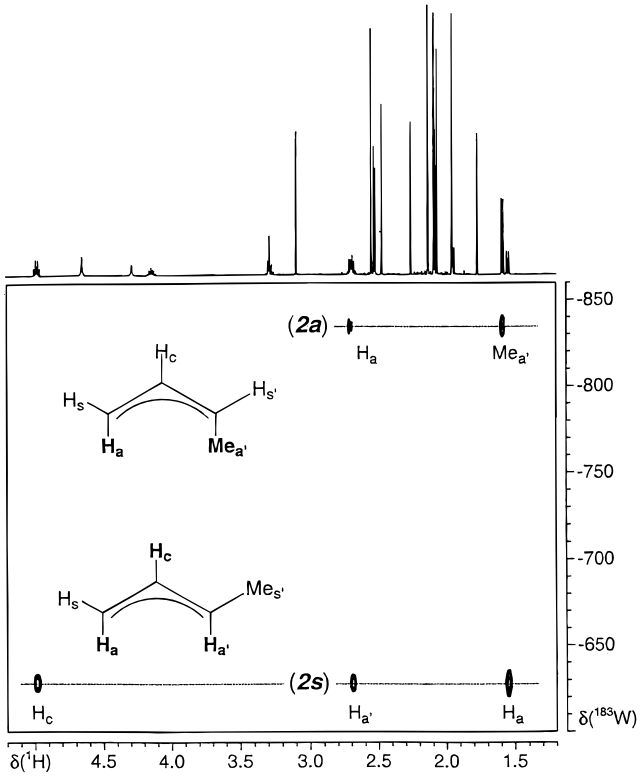

Figure 2. Section of the $^{183}W-^{1}H$ HMQC spectrum for a mixture of **2a** and **2s** showing the interactions of the metal spin with specific allyl protons in each isomer.

structure in which the allyl group is rotated ca. 120° with respect to a hypothetical *exo* rotamer, thereby bringing the *syn*-methyl group into the cleft defined by the two carbonyl ligands.

Single-Crystal X-ray Structural Characterization of the Orientational and Stereochemical Isomers of Tp′(CO)$_2$W(η^3-CH$_2$CHCHCH$_3$). Single crystals of **2a** suitable for X-ray analysis were obtained from recrystallization of a mixture of **2a** and **2s** in CH_2Cl_2/heptane; ^{1}H NMR spectroscopy showed that only **2a** was present in the crystallized material. The ORTEP representation of **2a** is shown in Figure 3, and selected bond distances and angles are given in Table 2. Considering the allyl ligand as a unit, the solid-state geometry can be described as pseudo-octahedral about the metal center. For purposes of discussion, the pyrazole rings next to the allyl will be termed the *cis*-pyrazoles and the remaining pyrazole ring the *trans*-pyrazole. The feature of note in the structure is the substantial twist of the allyl ligand away from a true *exo* orientation. The degree of rotation of the allyl (θ) can be defined as the dihedral angle between the allyl centroid, the central allyl carbon, the tungsten atom, and the OC−W−CO centroid. In an idealized *exo* orientation, θ would be 0°. The allyl group of **2a** is rotated 24° which allows the *anti*-methyl group to reside in the cleft formed by the two carbonyl groups, as predicted from the 2-D NOESY NMR.[21] The *anti*-methyl group is bent away from the plane of the allyl by 33.5°, much like the sister complex Tp(CO)$_2$Mo(η^3-*anti*-1-methylallyl) with its unsubstituted pyrazole rings.[23] The central carbon of the allyl is closest to the tungsten (W−C(4) = 2.229(9) Å), the unsubstituted carbon next (W−C(3) = 2.348(9) Å), and the *anti*-methyl-substituted carbon is furthest away (W−C(5) = 2.416 Å). As predicted by the infrared spectrum, the OC−W−CO bond angle is acute (80.5°).

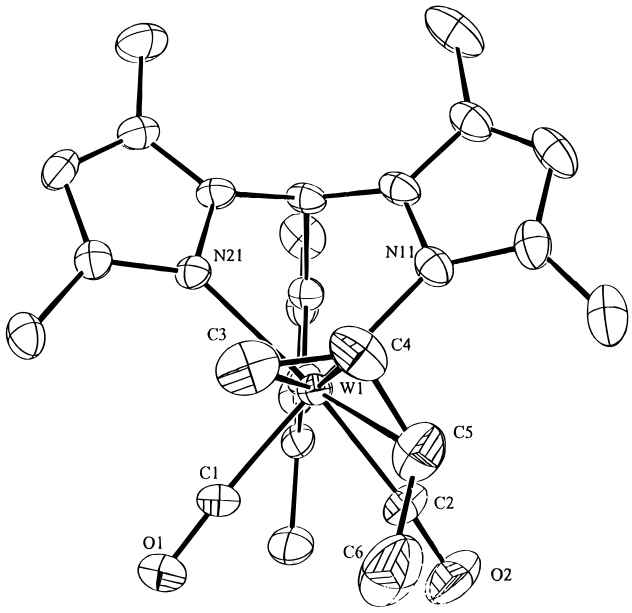

Figure 3. ORTEP of Tp′(CO)$_2$W(η^3-*anti*-1-methylallyl) (**2a**).

Table 2. Selected Bond Distances (Å) and Bond Angles (deg) for the *exo-Acute*-allyl Complexes[a]

	2a	7a	9
M(1)−C(1)	1.916(8)	1.931(6)	1.961(4)
M(1)−C(2)	1.950(8)	1.979(6)	1.930(4)
M(1)−C(3)	2.348(9)		2.370(5)
M(1)−C(4)	2.229(9)	2.422(6)	2.245(4)
M(1)−C(5)	2.416(10)	2.267(6)	2.363(4)
M(1)−C(6)		2.454(6)	
M(1)−N(11)	2.327(6)		2.215(3)
M(1)−N(21)	2.270(5)	2.309(5)	2.340(3)
M(1)−N(31)	2.196(10)	2.250(5)	2.289(3)
M(1)−N(41)		2.201(5)	
C(1)−O(1)	1.172(10)	1.169(7)	1.158(5)
C(2)−O(2)	1.160(10)	1.165(8)	1.159(5)
C(3)−C(4)	1.354(16)	1.515(9)	1.393(9)
C(4)−C(5)	1.423(16)	1.432(9)	1.379(8)
C(5)−C(6)	1.521(18)	1.369(9)	
C(6)−C(11)		1.525(9)	
C(1)−M(1)−C(2)	80.5(4)	81.2(2)	80.73(17)
C(1)−M(1)−N(11)	172.5(3)		87.08(15)
C(1)−M(1)−N(21)	92.9(3)	175.4(3)	94.89(15)
C(1)−M(1)−N(31)	94.2(3)	90.3(2)	162.25(15)
C(1)−M−(1)−N(41)		96.7(2)	
C(2)−M(1)−N(11)	95.7(3)		95.36(14)
C(2)−M(1)−N(21)	162.0(3)	96.6(2)	172.81(14)
C(2)−M(1)−N(31)	87.0(3)	157.0(2)	92.89(14)
C(2)−M(1)−N(41)		84.8(2)	
N(11)−M(1)−N(21)	88.76(22)		78.64(11)
N(11)−M(1)−N(31)	79.01(22)		76.98(11)
N(21)−M(1)−N(31)	76.70(19)	90.2(2)	89.64(11)
N(21)−M(1)−N(41)		79.0(2)	
N(31)−M(1)−N(41)		74.8(2)	
M(1)−C(1)−O(1)	176.5(7)	175.5(5)	175.4(4)
M(1)−C(2)−O(2)	175.3(9)	173.0(5)	175.3(3)
C(3)−C(4)−C(5)	114.7(9)	125.5(6)	114.7(5)
C(4)−C(5)−C(6)	125.3(10)	119.2(5)	
C(5)−C(6)−C(11)		120.7(5)	

[a] M = W for **2a** and **2s**; M = Mo for **9.** Numbers in parentheses are estimated standard deviations.

The *cis*-pyrazole rings of **2a** also undergo a distortion in response to allyl binding; they are twisted such that the boron and the tungsten lie on opposite sides of the ring planes. These distortions are also seen for **7a** and **9** (*vide infra*). Other researchers have noticed similar

Chart 2. Distortions of Pyazole Ligands

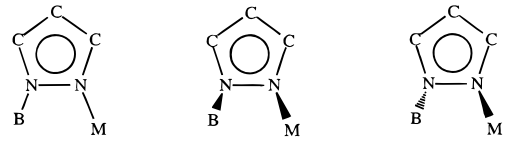

Table 3. Dihedral Angles Showing Distortions of Pyrazole Rings due to Interaction with Allyl Ligands[a]

	M−{N−N}−C dihedral angle			M−{N−N}−B dihedral angle		
	cis-L-pz	*cis*-R-pz	*trans*-pz	*cis*-L	*cis*-R	trans
2a	−176.6	173.9	177.9	16.0	−20.2	−5.8
7a	−169.1	173.6	175.4	20.6	−21.7	−12.1
9	−177.9	172.5	179.6	16.5	−19.2	−4.2

[a] For each complex, *cis*-L-pz is the *cis* oriented pyrazole ring opposite the direction of rotation of the allyl unit; *cis*-R-pz is the *cis* oriented ring in the direction of allyl rotation; *trans*-pz is the pyrazole ring *trans* to the allyl unit.

distortions in tris(pyrazolyl)borate complexes.[35−38] These distortions can be either a "tilting" of the pyrazole ring in which the metal and the boron remain on the same side of the pyrazole plane or a "twisting" of the pyrazole ring, such as described above (Chart 2). Typically, the C_3 symmetry of the tris(pyrazolyl)borate ligand is maintained, the "propeller" analogy holds. However, in **2a**, **7a**, and **9**, the rotational symmetry of the Tp′ ligand is destroyed as the *cis*-pyrazole rings are twisted in *opposite* directions. The overall effect is to push the leading edges of the *cis*-pyrazole rings outward in order to relieve steric congestion with the allyl ligand.

The M−{N−N}−C dihedral angle has been used to quantify both tilting and twisting distortions of the pyrazole rings.[35,36] Essentially, this is a measure of the displacement of the metal from the pyrazole plane and, hence, the effective overlap of a metal orbital with the sp^2 hybridized nitrogen. As such, the M−{N−N}−C dihedral angle would ideally equal 180°. However, this angle may underestimate the magnitude of a twisting distortion as the metal is not necessarily required to leave the plane of the pyrazole. Indeed, that is the case here as evaluation of the M−{N−N}−C dihedral angles for **2a**, **7a**, and **9** show that the metal is not significantly displaced from the pyrazole planes (Table 3). We feel that a more accurate measure of twisting distortions is found in the W−{N−N}−B dihedral angle. This dihedral angle would equal 0° for an undistorted geometry. Note that for a simple tilt of the pyrazole ring, this angle could remain unchanged. These angles are summarized in Table 3. In each case, the distortion of the *cis*-pyrazole ring in the direction of allyl rotation (*cis*-R-pz) is slightly larger and opposite in sign than is that of the ring away from the rotation (*cis*-L-pz).

X-ray quality single crystals of **2s** were obtained from one recrystallization in toluene/heptane, but all subsequent attempts resulted in crystalline mixtures of **2a** and **2s**. The refinement of the structure of **2s** was complicated by disorder with a pseudo mirror plane containing the boron atom, one pyrazole group, the tungsten atom, one carbonyl group, and the allyl methyl group. Both the allyl moiety and the other carbonyl group were disordered across the crystallographic mirror plane, with the unsubstituted allyl carbon coincident with the carbonyl carbon not in the mirror plane. The degree of disorder in the crystal limits the accuracy of the allyl carbon positions even though acceptable residuals were obtained. Selected bond distances and bond angles are given in Table 4. Regardless, the structure clearly shows the *syn* stereochemistry of the allyl moiety as predicted by the ^{1}H NOESY spectrum (Figure 4). Furthermore, the obtuse OC−W−CO angle (104.1°) is consistent with the infrared data. The *syn*-methyl group lies in the allyl plane, as is common.[23] There is a substantial rotation of the allyl fragment (ca. 114°) which places the *syn*-methyl group between the carbonyls. In contrast, the allyl unit in the related complex, Tp(CO)$_2$Mo(*syn*-1-ethylallyl), is rotated only 10° from an *exo* orientation and the *syn*-ethyl substituent lies between the pyrazole rings.[23] The methyl groups on the pyrazole rings in Tp′ must alter the steric profile of the ligand such that alkyl substituents cannot reside comfortably between the pyrazole rings.

Orientational isomerization in L$_2$XM(CO)$_2$(η^3-allyl) complexes has classically been defined as *endo* and *exo*, differing by a full 180°. The limitations of this model become apparent when comparing **2a** and **2s** as they

Table 4. Selected Bond Distances (Å) and Bond Angles (deg) for 2s

W(1)−C(1)	1.969 (12)	W(1)−N(11)	2.241 (6)
W(1)−C(2)	2.122 (14)	W(1)−N(11a)	2.241 (6)
W(1)−C(3)	2.273 (22)	W(1)−N(21)	2.258 (9)
W(1)−C(4)	2.314 (24)		
C(1)−W(1)−C(2)	104.1 (3)	C(1)−W(1)−N(21)	167.2 (5)
C(1)−W(1)−N(11)	87.4 (3)	N(11)−W(1)−N(21)	82.7 (2)

[a] Numbers in parentheses are estimated standard deviations.

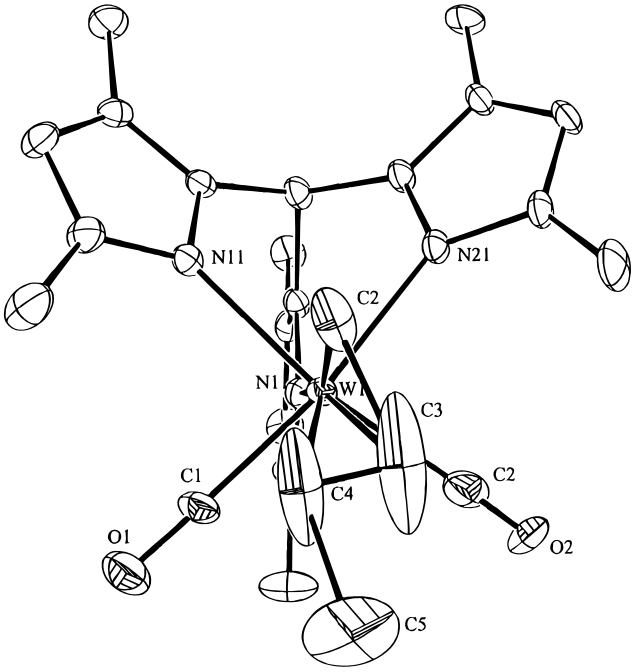

Figure 4. ORTEP of Tp′(CO)$_2$W(η^3-*syn*-1-methylallyl) (**2s**).

(35) Reger, D. L.; Collins, J. E.; Myers, S. M.; Rheingold, A. L.; Liable-Sands, L. M. *Inorg. Chem.* **1996**, *35*, 4904.
(36) Reger, D. L.; Collins, J. E.; Layland, R.; Adams, R. D. *Inorg. Chem.* **1996**, *35*, 1372.
(37) LeCloux, D. D.; Tokar, C. J.; Osawa, M.; Houser, R. P.; Keyes, M. C.; Tolman, W. B. *Organometallics* **1994**, *13*, 2855.
(38) Looney, A.; Han, R.; Gorrell, I. B.; Cornebise, M.; Yoon, K.; Parkin, G. *Organometallics* **1995**, *14*, 274.

Table 5. Selected ^{13}C NMR Data for Tp′(CO)$_2$M(η^3-allyl) Complexes[a]

	M	R	C^1	C^2	C^3	CO	CO
1	W	H	56.1 (t), $^1J_{CH}$ = 155	69.5 (d), $^1J_{CH}$ = 169		221.1, $^1J_{WC}$ = 160	
2a	W	*anti*-Me	54.7 (t), $^1J_{CH}$ = 160	70.9 (d), $^1J_{CH}$ = 167	65.1 (d), $^1J_{CH}$ = 160	224.0	220.2
2s	W	*syn*-Me	54.2 (t), $^1J_{CH}$ = 160	81.6 (d), $^1J_{CH}$ = 175	58.4 (d), $^1J_{CH}$ = 160	230.1, $^1J_{WC}$ = 160	228.6, $^1J_{WC}$ = 170
3a	W	*anti*-Et	54.6 (t), $^1J_{CH}$ = 157	69.1 (d), $^1J_{CH}$ = 166	72.3 (d), $^1J_{CH}$ = 153	223.6, $^1J_{WC}$ = 160	220.3, $^1J_{WC}$ = 170
3s	W	*syn*-Et	54.6 (t), $^1J_{CH}$ = 157	80.7 (d), $^1J_{CH}$ = 172	65.9 (d), $^1J_{CH}$ = 160	230.1, $^1J_{WC}$ = 160	228.8
4a	W	*anti*-Pr	55.5 (t), $^1J_{CH}$ = 156	69.5 (d), $^1J_{CH}$ = 166	70.6 (d), $^1J_{CH}$ = 150	223.5, $^1J_{WC}$ = 159	220.4, $^1J_{WC}$ = 164
4s	W	*syn*-Pr	54.5 (t), $^1J_{CH}$ = 156	81.2 (d), $^1J_{CH}$ = 173	64.1 (d), $^1J_{CH}$ = 157	230.3, $^1J_{WC}$ = 156	228.7, $^1J_{WC}$ = 174
5a	W	*anti*-Bz	54.8 (t), $^1J_{CH}$ = 158	68.7 (d), $^1J_{CH}$ = 167	70.7 (d), $^1J_{CH}$ = 160	223.4, $^1J_{WC}$ = 160	220.2, $^1J_{WC}$ = 150
5s	W	*syn*-Bz	55.0 (t), $^1J_{CH}$ = 157	81.1 (d), $^1J_{CH}$ = 173	63.2 (d), $^1J_{CH}$ = 159	229.7, $^1J_{WC}$ = 150	228.4, $^1J_{WC}$ = 170
9	Mo	H	63.5	80.2		229.5	
10a	Mo	*anti*-Me	63.5 (t), $^1J_{CH}$ = 160	82.0 (d), $^1J_{CH}$ = 161	73.7 (d), $^1J_{CH}$ = 153	232.7	228.6
10s	Mo	*syn*-Me	65.1 (t), $^1J_{CH}$ = 159	89.1 (d), $^1J_{CH}$ = 165	68.2 (d), $^1J_{CH}$ = 162	235.0	234.4

[a] Spectra recorded at 100 MHz in C_6D_6. Chemical shifts given in ppm; coupling values given in Hz.

Chart 3. Orientational Isomers for Tp′(CO)$_2$W(η^3-CH$_2$CHCHR) Complexes[a]

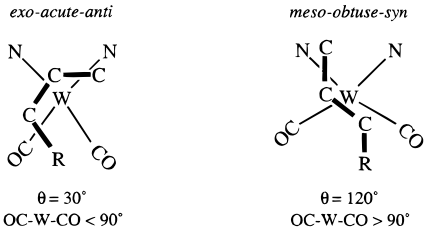

[a] View is down the allyl−metal axis; allyl hydrogens and off-equatorial plane atoms have been omitted for clarity.

differ by approximately 90° (ca. 30° vs 120°). If the *exo* notation is retained for the 30° allyl rotamer, we propose that the complementary allyl isomer be designated as *meso* from the Greek *mesos* meaning "mid". The *meso* nomenclature highlights the orthogonal relationship of the two rotamers. Given the crucial role of the *cis*-carbonyl ligands in the orientation of the allyl (see EHMO calculations discussion), we favor adding an angle designator to specify the OC−M−CO angle; *exo-acute* and *meso-obtuse* would convey the essential geometric information (Chart 3).

General NMR Spectroscopic Features of Tp′(CO)$_2$W(η^3-allyl) Complexes. The pyrazole protons of the parent allyl complex, **1**, revealed an effective mirror plane for the complex in solution. The *syn* protons were located at 3.36 ppm, the central proton at 3.17 ppm, and the *anti* protons were upfield at 1.97 ppm. Coupling constant values among the allyl protons were normal: $^3J_{ac}$ = 9.4 Hz and $^3J_{sc}$ = 6.6 Hz. The ^{13}C NMR spectrum of **1** showed equivalent terminal carbons at 56.1 ppm and the unique, central allyl carbon at 69.5 ppm.

With the structural data in hand, the NMR behavior of the substituted allyl complexes can be better understood. The central protons for the **s** isomers (5−5.2 ppm) experience a downfield shift of nearly 2 ppm relative to those of the **a** isomers (3.2 ppm), which is similar to those of the parent complex. A similar downfield shift (11 ppm) is experienced by the central carbons of the **s** isomers as well (Table 5). Inspection of the crystal structure of **2s** shows that the central allyl portion of **2s** lies near the plane of the closest *cis*-pyrazole. A deshielding effect due the edge-directed approach to the aromatic ring would be expected. Similar positions are adopted by H_a and H_s′ on **2a**; these signals were found downfield of what is expected based on comparision to the parent complex. In contrast, both H_a and H_s for the **s** isomers are shielded (0.4 and 2.4 ppm, respectively) relative to **1** due to their positions above the pyrazole rings. By way of comparision, allyl

Figure 5. Orientational isomers for Tp′(CO)W(η^3-*syn*-1-phenylallyl) (**6**). View is down the allyl−metal axis; off-equatorial plane atoms have been omitted for clarity.

protons in Cp−allyl systems are uniformly shielded by proximity to the ligand ring.[6]

It was noted earlier that the $^3J_{HH}$ coupling constant values among the allyl protons for the **s** isomers do not adequately convey stereochemical information. The perturbed coupling values for the *meso-syn* isomers may be due to the distortions necessary to accomodate a *syn*-substituted allyl in the Tp′(CO)$_2$W ligand sphere. This may also account for the lack of observable geminal and homoallylic coupling in the **s** isomers. The lower energy carbonyl stretches along with the higher $^1J_{WC}$ coupling constant values seen for the carbonyl groups of the **s** isomers support the above model, since distortions in the allyl fragment should inhibit the allyl's acceptance of back-bonding electrons from the metal, thus, favoring back-donation into the carbonyl ligands.

Variable-Temperature ^{1}H NMR Study of Tp′(CO)$_2$W(CH$_2$CHCHPh).[62] In an earlier study, the solid-state structure of the 1-*syn*-phenylallyl complex, **6**, was shown to be similar to that of the *anti*-alkyl-substituted allyls whereas the solution structure corresponds more closely to the conformation adopted by the *syn*-alkyl-substituted allyls (Figure 5).[21] Notably, the room-temperature ^{1}H NMR spectrum of **6** is strongly reminiscient of those of the *meso-syn* alkylallyl isomers. The ^{1}H NMR spectrum at −90 °C differs markedly from the room-temperature spectrum. A ^{13}C NMR spectrum obtained at low temperature also supports the presence of two allyl isomers for **6** (see Experimental Section).

The variable-temperature NMR behavior of **6** is reversible, and we believe the spectrum at room temperature represents the average of spectra for two distinct isomers which are partially resolved at −110 °C. Phase-sensitive 2-D ^{1}H NOESY and selective magnetization transfer experiments had previously ruled out *syn-anti* exchange at room temperature.[21] The resonance signals for H_a′ showed minimal interference over most of the temperature range; this signal allowed extraction of data relevant to thermodynamic parameters for the isomerization process.

Equilibrium ratios from the slow exchange (−90 to −120 °C) region were determined by integration of the

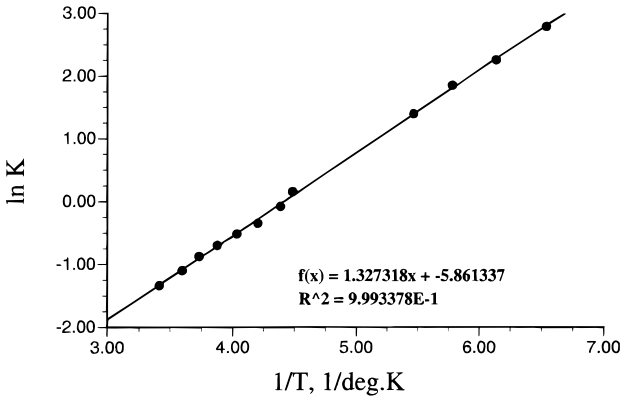

Figure 6. Arrhenius plot for Tp′$(CO)_2$W(η^3-*syn*-1-phenyl allyl) (**6**).

partially resolved peaks. Equilibrium ratios of the two isomers in the fast exchange (−35 °C to 20 °C) and the coalescence (−45 to −50 °C) regions were determined by assuming that the average chemical shifts reflected the fractional mole ratios referenced to fixed chemical shift values, as determined by the low-temperature limit. An Arrhenius plot (Figure 6) yielded equilibrium values of 2.7 kcal mol^{-1} for $\Delta H°$ and 11.6 cal mol^{-1} K^{-1} for $\Delta S°$. An average value for the activation energy linking these two isomers, $\Delta G^{\neq}$, of 10.4 kcal mol^{-1} was also obtained.

One attractive hypothesis is that the predominant isomer at room temperature resembles the structure based on 2-D ^{1}H NOESY data, while the low-temperature isomer resembles the solid-state structure. Molecular mechanics calculations based on a model derived from the X-ray structure estimate a barrier to phenyl ring rotation of over 80 kcal mol^{-1} when the phenyl group is between the pyrazole rings; the high barrier is primarily due to one of the *cis*-methyl groups of the pyrazole. Therefore, a mechanism involving simple rotation about the metal−allyl axis is unlikely as the phenyl group would be required to "pass through" the *cis*-methyl group of the pyrazole. A $\eta^3-\eta^1-\eta^3$ mechanism is proposed in which rotation about the metal−carbon bond in the η^1 form occurs (Scheme 2). This would account for both the lack of exchange of H_a and H_s and for the retention of the *syn* position for the phenyl group.

The above rotamer assignments imply that the conformer in which the phenyl ring is between the pyrazole rings (clearly an unfavorable steric environment) is enthalpically preferred. This arene to pyrazole geometric relationship is a common feature of tris(pyrazolyl)borate group VI metal compounds which contain phenyl-substituted four-electron donor alkyne ligands.[20,39−41] It has been noted that phenyl rings favor this position more than hydrogen atoms, alkyl groups, or heteroatoms with lone pairs.[42] The solid-state structure of **6** also appears to be the ground-state geometry of choice for *syn*-phenyl-substituted tris(pyrazolyl)borate dicarbonyl group VI metal complexes.[21−23] Guidelines developed

Scheme 2

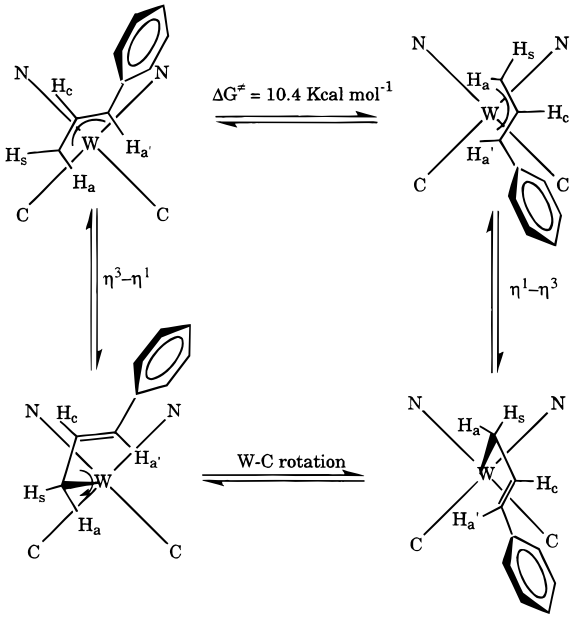

for aromatic−aromatic interactions[43] suggest that the enthalpic stabilization for the phenyl group is due to favorable CH−π interactions with both *cis*-pyrazole rings.

The $\Delta S°$ of 11.6 cal mol^{-1} K^{-1} is unusually large for an intramolecular isomerization process; these values tend to be on the order of ±5 cal mol^{-1} K^{-1}.[44] Phenyl rotation in the high-temperature form will contribute to the entropy term since free rotation in the ground state appears to have a substantial barrier. Using parameters derived from the X-ray structure, the rotational contribution to the entropy (S_{rot}) due to a freely rotating phenyl ring was calculated.[45] A value for S_{rot} of 15.7 cal mol^{-1} K^{-1} was obtained, which is roughly comparably to the measured $\Delta S°$. Overall, the interconversion process is entropically driven and can be summarized by three points: (1) At low temperatures, the isomer of lower entropy predominates. The rate of isomerization is slow, although not frozen out completely, on the NMR time scale. (2) As the temperature is raised, the equilibrium shifts as the entropic contribution becomes more important. Thermal energy becomes sufficient to allow interconversion of the isomers on the NMR time scale. (3) At high temperatures, rapid exchange between both isomers occurs. The predominant species becomes the one with the phenyl ring located between the carbonyl ligands.

Characterization of Tp′$(CO)_2$W(CHRCHCHR′) Complexes. A *syn*-phenyl configuration for both isomers of the disubstituted 1-phenyl-3-methyl complex, **7**, is proposed. This assignment is based on (1) the known preference of the phenyl group for a *syn*-position[21−23] and (2) comparison to the chemical shifts and coupling constants of the monosubstituted complexes. An *anti* position for the methyl group of **7a** and a *syn* position for the methyl group of **7s** were indicated

(39) Caldarelli, J. L.; White, P. S.; Templeton, J. L. *J. Am. Chem. Soc.* **1992**, *114*, 10097.
(40) Collins, M. A.; Feng, S. G.; White, P. S.; Templeton, J. L. *J. Am. Chem. Soc.* **1992**, *114*, 3771.
(41) Feng, S. G.; Philipp, C. C.; Gamble, A. S.; White, P. S.; Templeton, J. L. *Organometallics* **1991**, *10*, 3504.
(42) Philipp, C. C.; Young, C. G.; White, P. S.; Templeton, J. L. *Inorg. Chem.* **1993**, *32*, 5437.
(43) Hunter, C. A.; Sanders, J. K. M. *J. Am. Chem. Soc.* **1990**, *112*, 5525.
(44) Mann, B. E. Non-rigidity in Organometallic Complexes. In *Comprehensive Organometallic Chemistry*; Wilkinson, G., Stone, F. G. A., Abel, E. W., Eds.; Pergamon: New York, 1982.
(45) Barrow, G. M. *Physical Chemistry*, 5th ed.; McGraw-Hill: New York, 1988.

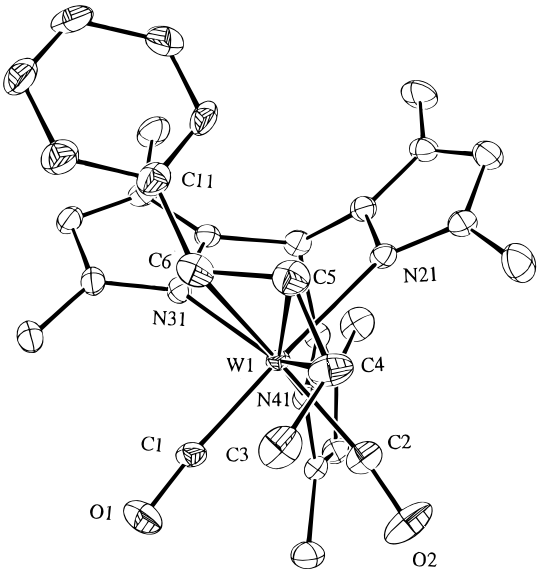

Figure 7. ORTEP diagram of Tp′$(CO)_2$W(η^3-*syn*-1-phenyl-*anti*-3-methylallyl) (**7a**).

by comparison of the chemical shifts to those of **2a** and **2s**, respectively. The ^{1}H NMR spectrum of **7** revealed strong downfield shifts for all allyl protons.

Recrystallization of a mixture of the isomers of the 1-phenyl-3-methylallyl complex, **7**, produced single crystals of the **a** isomer. The structure of **7a** confirms the 1-*syn*-phenyl-3-*anti*-methyl stereochemistry. The allyl is rotated by 38°, which places the *syn*-phenyl substituent between the pyrazole rings and the *anti*-methyl group in the cleft formed by the carbonyl groups (Figure 7). The relevant W−{N−N}−B dihedral angles are 20.6° and −21.7°.

The metal−carbon bond lengths to the terminal allyl carbons (W−C(4) = 2.422(6) Å; W−C(6) = 2.454(6) Å) exceed the distance to the central carbon (W−C(5) = 2.267(6) Å). The bond length from the central carbon of the allyl to the methyl-substituted allyl carbon (C(4)−C(5) = 1.432(9) Å) is substantially longer than that to the phenyl-substituted allyl carbon (C(5)−C(6) = 1.369-(9) Å). This is indicative of distortion toward an η^1-bound form in which the methyl-substituted carbon remains bound to the metal as the phenyl-substituted carbon approaches sp^2 hybridization.[23] An $\eta^3-\eta^1-\eta^3$ process would provide a route for *syn*/*anti* interconversion of the methyl group while retaining the phenyl group in a *syn* position (Scheme 3).

In contrast to the monoalkyl-substituted allyl complexes, the 1-ethyl-3-methylallyl complex **8** is fluxional on the NMR time scale. At −70 °C the two isomers, **8x** and **8y**, are reasonably well-resolved. The downfield shifts seen for the central allyl protons and for the central allyl carbons suggest *meso* orientations for both isomers. This limits the stereochemical choices for the allyl to *syn*/*syn* and *syn*/*anti* since it is unlikely that an *anti*/*anti* configuration could be accommodated in a *meso* orientation. By necessity, one allyl terminus would be located between the *cis*-pyrazole rings. Herein lies the root of the configurational lability of the allyl fragment: an alkyl group has difficulty residing between the *cis*-pyrazole rings. Note that for complex **7** it is the phenyl group with its favorable arene/pyrazole CH−π interaction which sits between the *cis*-pyrazole rings for both **7a** and **7s**. The variable-temperature

Scheme 3

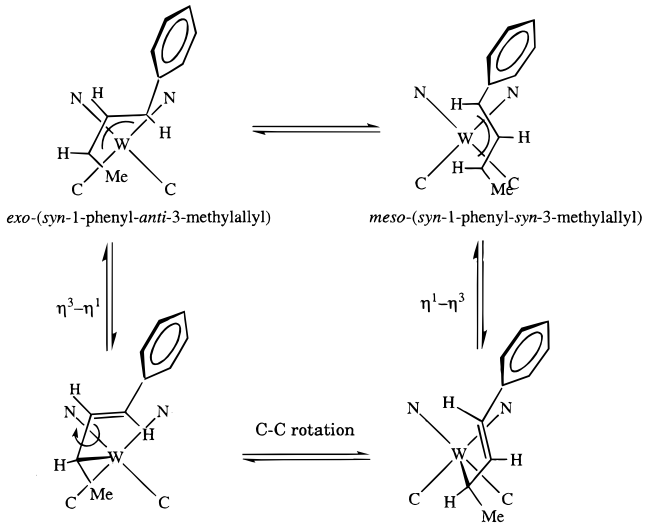

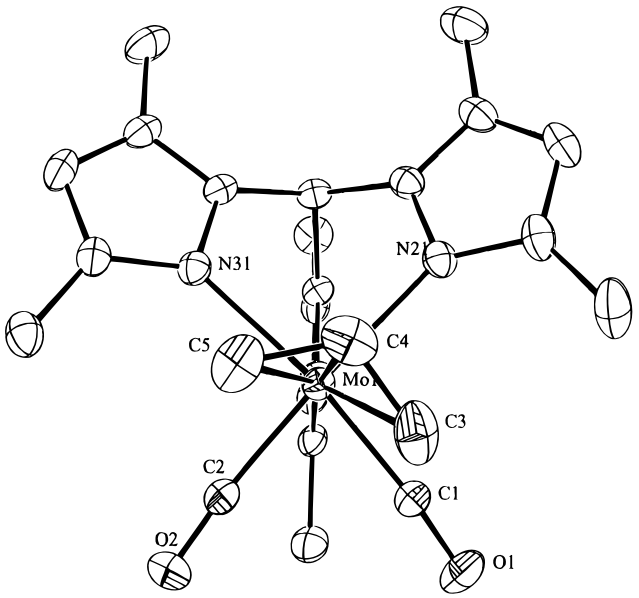

Figure 8. ORTEP diagram of Tp′$(CO)_2$Mo(η^3-C_3H_5) (**9**).

behavior of **8** allows the estimation of a barrier to interconversion on the order of 12 kcal/mol.

Characterization of Tp′$(CO)_2$Mo(η^3-allyl) Complexes. The parent allyl complex, **9**, has been known for almost 30 years,[1] and the synthesis of the 1-methyl-substituted complex, **10**, was recently reported in the literature.[22] NMR data for **9** and **10** were obtained in C_6D_6 to allow direct comparison of chemical shift values with the tungsten analogues. In contrast to the tungsten case, the central proton of **9** was located furthest downfield (4.03 ppm) as a triplet of triplets with $^3J_{ac}$ = 10 Hz and $^3J_{sc}$ = 6.4 Hz. The *syn* protons (3.57) were found downfield of the *anti* protons (1.88).

A single-crystal X-ray study of **9** defined the orientation of the allyl ligand relative the to Tp′$(CO)_2$M fragment as *exo-acute* (Figure 8). The allyl fragment is rotated 21°, and the OC-Mo−CO angle is 80.7°. The allyl fragment in the unsubstituted Tp complex, Tp-$(CO)_2$Mo(η^3-C_3 H_5), exhibits only a 6° rotation,[23] and the isoelectronic Cp$(CO)_2$Mo(η^3-C_3H_5) is rigorously *exo* in the solid state.[9] The Mo-{N-N}-B dihedral angles are −19.2° and 16.5° for the *cis*-pyrazole rings. The *trans*-pyrazole shows only a nominal distortion of −4.2°. The

related complexes $Tp(CO)_2Mo(\eta^3\text{-}C_3H_4R)$ (R = H, 2-Me) exhibit smaller distortions of only 0−8° for all relevant dihedral angles. The tris(pyrazolyl)gallate complex, $Gp(CO)_2Mo(\eta^3\text{-}C_3H_5)$ ($Gp = MeGa(N_2C_3H_5)_3$), where the Gp ligand is more sterically bulky than is the unsubstituted (pyrazolyl)borate ligand,[46] shows Mo−{N−N}−B dihedral angles of 18.2° and −18.2° for the *cis*-pyrazoles and 5.2° for the *trans*-pyrazole.

The central carbon of the allyl fragment, C(4), is closest to the metal (Mo−C(4) = 2.245(4) Å). This tips the plane of the allyl toward the metal, as is common.[47] The terminal carbons are nearly equidistant from the molybdenum center (Mo−C(3) = 2.370(5) Å, Mo−C(5) = 2.363(4) Å). Bond distances within the allyl fragment approach typical distances for a carbon−carbon double bond (C(3)−C(4) = 1.393(9) Å, C(4)−C(5) = 1.379(8) Å), and the C(3)−C(4)−C(5) bond angle is 114.7(5)°, reflecting sp^2 hybridization. The room-temperature ^1H NMR spectrum of **9** implies the existence of an effective mirror plane in solution. The solution symmetry was retained even to −90 °C. Either a θ value near 0° in solution or a low-energy rocking motion in accord with the low barrier (~1 kcal) estimated by the EHMO calculations is compatible with the data (see below).

Examination of the ^1H NMR spectrum of **10** showed the presence of two isomers (**10a** and **10s**). As in the tungsten complexes, patterns appearing to be simple doublets of triplets indicative of *anti* substitution were obtained for each of the central allyl protons. The similarities between the molybdenum and tungsten complexes prompt the assignment of **10a** as the *anti*-methylallyl complex and **10s** as the *syn*-methylallyl complex. This is in accord with the assignments of Joshi *et al.*[22] A unit cell determination was performed on a single crystal of **10a**. The obtained unit cell parameters for **10a** were compared to those of **2a**. The close correspondence between the two suggested that **10a** possessed the same geometry in the solid state as does **2a** (*exo-acute-anti*), and a full structure determination was not undertaken. The ^{13}C NMR spectrum of **10** revealed downfield shifts for the allyl carbons relative to the tungsten complexes.

Extended Hückel Molecular Orbital (EHMO) Calculations. Molecular orbital studies of d^4 transition metal allyl complexes have focused upon stereochemical preferences and the regioselectivity of their reactions with nucleophiles. Schilling, Hoffman, and Faller calculated a high (46 kcal/mol) barrier to allyl rotation and a slight preference for an *endo* conformation for $Cp(CO)_2Mo(\eta^3\text{-allyl})$ complexes.[48] For the more general $L_3(CO)_2Mo(\eta^3\text{-allyl})$ case, Curtis and Eisenstein found the *exo* rotamer to be preferred by 10−15 kcal/mol.[49] The OC−M−CO angle was fixed at 90° for these molecular orbital studies. Crystallographic studies of d^4 dicarbonyl group VI metal η^3-allyl complexes containing anionic, tridentate ligands reveal acute OC−W−CO bond angles in all cases.[9,21−23,29,46,50−53] A correlation exists between the OC−W−CO bond angle and the orientation of single-faced π-donors for d^4 dicarbonyl transition metal complexes.[54] It was thought that the same molecular orbital principles would prove useful in understanding the orientational isomerization exhibited by these allyl complexes.

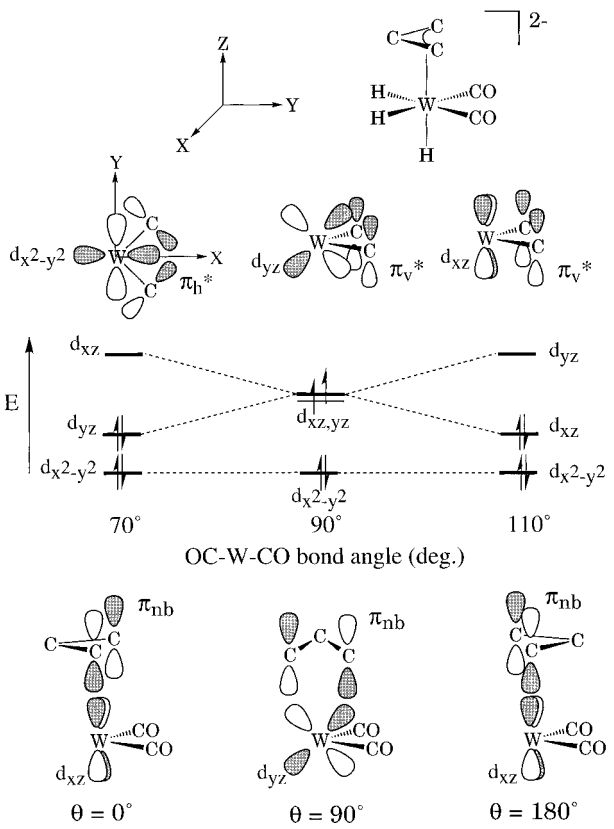

Figure 9. Metal dπ interactions with *cis*-dicarbonyl ligands, qualitative diagram of MO dependence on OC−W−CO angle, and metal dπ interactions with the allyl π-nonbonding orbital.

Details regarding the bonding in allyl complexes have been discussed at length.[48,49,55] Our concern here is the interplay between allyl orientation and the OC−W−CO angle, and the orbitals of interest are the allyl π-nonbonding (π_{nb}) orbital and those metal orbitals derived from the octahedral t_{2g} dπ set. In the coordinate system used, rotated 45° in the *xy* plane relative to conventional axes, the metal dπ orbitals are $d_{x^2-y^2}$, d_{xz}, and d_{yz}. The energy of these dπ levels is coupled to the angle between *cis*-carbonyl ligands.[54,56] With four dπ electrons in a diamagnetic octahedral complex, two of the dπ orbitals will be filled and one will remain empty. It is the empty dπ orbital with which the allyl π_{nb} orbital must find a match (Figure 9). An allyl orientation of either 0° or 180° will merge with an acute OC−W−CO angle and favor an empty d_{xz} orbital. An allyl rotation of 90° should complement an obtuse OC−W−CO angle, and an empty d_{yz} should result.

Three facial hydride ligands were used in place of the Tp′ ligand, with the remaining sites occupied by two

(46) Breakell, K. R.; Rettig, S. J.; Singbeil, D. L.; Storr, A.; Trotter, J. *Can. J. Chem.* **1978**, *56*, 2099.
(47) Green, M. L. H.; Nagy, P. L. I. *Adv. Organomet. Chem.* **1964**, *2*, 325.
(48) Schilling, B. E. R.; Hoffman, R.; Faller, J. W. *J. Am. Chem. Soc.* **1979**, *101*, 592.
(49) Curtis, M. D.; Eisenstein, O. *Organometallics* **1984**, *3*, 887.
(50) Breakell, K. R.; Rettig, S. J.; Storr, A.; Trotter, J. *Can. J. Chem.* **1979**, *57*, 139.
(51) Chong, K. S.; Rettig, S. J.; Storr, A.; Trotter, J. *Can. J. Chem.* **1979**, *57*, 1335.
(52) Holt, E. M.; Holt, S. M.; Waston, K. J. *J. Chem. Soc., Dalton Trans.* **1973**, 2444.
(53) Kosky, C. A.; Ganis, P.; Avitabile, G. *Acta Crystallogr.* **1971**, *B27*, 1859.
(54) Templeton, J. L.; Caldarelli, J. L.; Feng, S. G.; Phillips, C. C.; Wells, M. B.; Woodworth, B. E.; White, P. S. *J. Organomet. Chem.* **1994**, *478*, 103.
(55) Clarke, H. L. *J. Organomet. Chem.* **1974**, *80*, 155.
(56) Kubacek, P.; Hoffman, R. *J. Am. Chem. Soc.* **1981**, *103*, 4320.

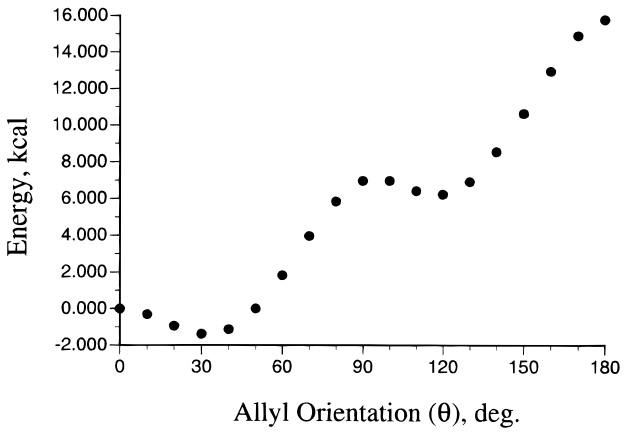

Figure 10. Configuration energy vs allyl orientation for $[H_3W(CO)(\eta^3\text{-}C_3H_5)]^{2-}$. The OC−W−CO angle was held at 90° for this data set. The zero of the energy scale was set at $\theta = 0°$.

carbonyl ligands and a symmetric allyl group positioned parallel to the OC−W−CO plane. The allyl moiety in $[H_3(CO)_2W(\eta^3\text{-}C_3H_5)]^{2-}$ was rotated in 10° increments from an *exo* orientation ($\theta = 0°$) to an *endo* orientation ($\theta = 180°$). For each allyl orientation, the OC−W−CO angle was varied from 70° to 110° in 4° steps. Extended Hückel molecular orbital calculations were performed for each of these 209 geometries.

The OC−W−CO angle of minimum energy varied systematically with allyl rotation. For $\theta = 0°$, the total energy minimized at an acute OC−W−CO angle of 82°. As the allyl was rotated, the OC−W−CO angle of minimum energy climbed steadily to an obtuse angle of 98° for an allyl orientation of $\theta = 90°$. The OC−W−CO angle of minimum energy then declined to 84° at the *endo* orientation with $\theta = 180°$. Indeed, allyl rotation is coupled with variations in the OC−W−CO angle.

The total energy rose 6 kcal when the allyl was rotated 90°. The *endo* allyl orientation ($\theta = 180°$) was 16 kcal mol^{-1} above the *exo* orientation ($\theta = 0°$), confirming the results of Curtis and Eisenstein. Surprisingly, the global minimum was located at an allyl orientation of 30° rather than at 0° (Figure 10). A double minimum with a barrier on the order of 1 kcal is implied by the mirror symmetry of the model. A second even more shallow (0.3 kcal mol^{-1}) local minima was located at $\theta = 120°$. These exceedingly small stabilizations may couple with steric effects created by terminal substitution on the allyl to allow observation of distinct isomers. The stabilizations seen at $\theta = 30°$ and 120° are independent of variations in the OC−W−CO angle; allowing the OC−W−CO angle to flex during allyl rotation only "softens" the orientation−energy profile.

Conclusions

Terminal alkyl substitution on the allyl portion of Tp′-$(CO)_2W(\eta^3$-allyl) complexes creates an orientational and geometric interdependence with allyl stereochemistry. Allyl moieties with *anti*-alkyl substituents approximate *exo* orientations with acute OC−W−CO angles. *syn*-alkylallyls are rotated 90° from their *anti* analogs. These *meso* rotamers are also distinguished by obtuse OC−W−CO angles. EHMO calculations on the model complex, $[H_3(CO)_3W(\eta^3\text{-}C_3H_5)]^{2-}$, reveal small electronic minima corresponding to the two orientations due to rotation of the allyl unit. Experimentally, simple rotation of the allyl fragment is not operative in either the alkyl- or aryl-substituted complexes, as $\eta^3-\eta^1-\eta^3$ processes are indicated for isomer interconversion. However, the EHMO calculations do show the possibility for allyl isomers differing by 90° and the dependence of the OC−W−CO angle on the allyl orientation. The observed orientational and stereochemical preferences for $L_2X(CO)_2M(\eta^3$-allyl) (M = Mo, W) complexes can be explained as the overlay of steric factors onto the electronic manifold. In Cp−allyl systems, *syn*-alkyl substitution is almost exclusively preferred and both *endo* and *exo* orientations are known for simple alkyls, with the *endo* orientation favored electronically.[5,6] With the larger Cp* ligand (Cp* = pentamethylcyclopentadienyl), both *syn* and *anti* geometries are possible, but only the *exo* orientation is seen for substituted allyls.[29] In Tp−allyl systems, *anti*-alkyl substitution is dominant and both *syn*- and *anti*-alkylallyls are accomodated in an *exo* orientation which is electronically preferred.[23] With the larger Tp′ ligand, *syn*-alkyl substitution is preferred due to the *cis*-pyrazole 3-methyl groups. Note that Liebeskind and co-workers have documented a ground-state rehybridization from an η^3-bonding mode toward an η^1-bonding mode for *syn*-alkylallyls in the Tp system due to close contacts between the *syn* substituent and the forward carbon of one of the *cis*-pyrazole groups.[23] In order to minimize both allylic strain and steric contacts, *syn*-alkylallyls in Tp′$(CO)_2W(\eta^3$-allyl) complexes must adopt a *meso* orientation which corresponds to the local minimum seen at $\theta = 120°$.

Experimental Section

General Methods. Manipulations involving air-sensitive reagents were performed under a dry nitrogen atmosphere with standard Schlenk techniques. Solvents were purified as follows: methylene chloride was distilled from P_2O_5; Et_2O, THF, and hexanes were distilled from sodium benzophenone ketyl; toluene was distilled from sodium; acetonitrile was distilled from CaH; other solvents were used as obtained from commercial sources. Tp′$(CO)_3WH$ was prepared according to published procedures;[1] $(CH_3CH_2CN)_3W(CO)_3$ was prepared following the procedure of Kubas;[57] alkyne complexes of the form [Tp′$(CO)_2W(RC{\equiv}CR)$][OTf]were prepared by a literature route,[41] except that AgOTf (OTf = trifluoromethanesulfonate) was used in place of $AgBF_4$; other reagents were used as obtained from commercial sources.

Photolyses were performed with a Hanovia 450 W medium-pressure Hg arc lamp at ambient temperatures. Photolysis vessels were sealed with septa, and the solutions were stirred during irradiation. Infrared spectra were recorded at 4 cm^{-1} resolution. Conventional and low-temperature NMR spectra were recorded at 400 MHz. When necessary, homonuclear decoupling experiments (400 MHz) were used to extract coupling constants from ^1H NMR spectra. Two-dimensional NMR spectra for a mixture of **2a** and **2s** were obtained on a Bruker AMX-500 (500 MHz) spectrometer. A phase-sensitive $^1H\{^{11}B\}$ NOESY spectrum was recorded using the conventional pulse sequence with a mixing time of 600 ms. Additionally, continuous wave ^{11}B decoupling was applied to the Tp′ resonances. $^{183}W-^1H$ and $^{15}N-^1H$ HMQC spectra were obtained as previously described using $D = 50$ and 80 ms, respectively.[21] The ^{11}B, ^{183}W, and ^{15}N spectra were referenced relative to $BF_3{\cdot}Et_2O$, WF_6, and CH_3NO_2, respectively. Mi-

(57) Kubas, G. J.; Van Der Sluys, L. S. *Inorg. Synth.* **1990**, *28*, 29.

croanalyses were performed by Atlantic Microlab, Inc., Norcross, GA, unless otherwise noted.

Tp′(CO)$_2$M(η^3-CH$_2$CHCHR). These compounds were synthesized by various methods. Representative examples for each method are given below. Due to the large volume of data, full ^{1}H and ^{13}C spectroscopic characterization for the monosubstituted allyl complexes is provided in the Supporting Information. For relevant ^{1}H NMR and ^{13}C NMR data, refer to Tables 1 and 4.

Tp′(CO)$_2$W(η^3-CH$_2$CHCH$_2$) (1). Method A:[26] A solution containing 2.00 g (4.89 mmol) of (CH$_3$CH$_2$CN)$_3$W(CO)$_3$ in 80 mL of THF was prepared. The mixture turned dark brown upon heating to 60 °C. An immediate efflux of gas (CO) was noted upon the addition of a 3-fold excess of allyl chloride (1.20 mL, 14.7 mmol). After 15 min, the IR spectrum of the solution showed that no starting material remained. While the solution temperature was maintained at 60 °C, 1.68 g (5.00 mmol) of KTp′ was added under positive nitrogen flow. The IR spectrum after 5 min showed absorbances corresponding to the η^3-allyl product. The solution was stirred for 30 min to ensure complete reaction. At this point, the solvent was removed and the residue was chromatographed on alumina with CH$_2$Cl$_2$ as the eluent. An orange-yellow band was collected. Removal of solvent yielded 1.76 g (62%) of an orange-yellow solid. IR (KBr, cm^{-1}): ν_{BH} 2548; ν_{CO} 1919, 1817; ν_{CN} 1547. Anal. Calcd for WC$_{20}$H$_{27}$N$_6$BO$_2$: C, 41.55; H, 4.71; N, 14.54. Found: C, 41.48; H, 4.69; N, 14.53.

Tp′(CO)$_2$W(η^3-CH$_2$CHCHMe) (2a,s). Method A with crotyl chloride as the allylic substrate; yellow-orange, 55%. Method B: A solution containing 1.00 g (1.77 mmol) of Tp′(CO)$_3$WH and 0.30 mL (3.83 mmol) of 2-butyne in 130 mL of THF was prepared. After 45 min of irradiation, the IR spectrum of the solution showed peaks corresponding to an η^2-vinyl intermediate (1937, 1846 cm^{-1}), the η^3-allyl product (1921, 1823 cm^{-1}), and remaining starting material (1992, 1904, 1868 cm^{-1}). The reaction was complete after 2 h, and only the η^3-allyl product was evident in the IR spectrum. The solvent was removed, and the oily, brown residue was chromatographed on alumina with CH$_2$Cl$_2$ as the eluent. A brown-yellow band was collected. The solvent was removed, and the residue was treated with 4 mL of CH$_2$Cl$_2$. The solution was filtered to leave behind 0.31 g of a bright yellow powder (100% isomer **2a** by ^{1}H NMR). The filtrate was loaded onto an alumina column, and a yellow band was eluted with hexanes:CH$_2$Cl$_2$ (5:1). Removal of solvent and a hexanes wash produced 0.15 g of an orange solid (85% isomer **2a** by ^{1}H NMR). The overall yield for Method B was 44% (96% **2a**, 4% **2s**). Isomer **2a** has been synthesized previously through hydride addition to a cationic 2-butyne complex.[20] IR (KBr, cm^{-1}): **2a** ν_{BH} 2548; ν_{CO} 1910, 1815; ν_{CN} 1545; **2s** ν_{BH} 2540; ν_{CO} 1919, 1819; ν_{CN} 1549. ^{11}B NMR (δ, C$_6$D$_6$, 160.5 MHz): **2a**, **2s** −8.9. ^{15}N NMR (δ, C$_6$D$_6$, 50.7 MHz): **2a** −154.9, −156.0, −157.6 (N$_1$), −132.6, −133.5, −134.1 (N$_2$); **2s** −156.2, −157.3, −158.5 (N$_1$), −139.6, −146.3, −150.3 (N$_2$). ^{183}W NMR (δ, C$_6$D$_6$, 20.8 MHz): **2a** 838; **2s** 628.

Tp′(CO)$_2$W(η^3-CH$_2$CHCHEt) (3a,s). This complex was prepared by Method B with 1,4-pentadiene as the substrate and a photolysis time of 2.5 h. The orange product was obtained in 40% yield. IR (KBr, cm^{-1}): ν_{BH} 2558; ν_{CO} 1914, 1815; ν_{CN} 1545. Anal. Calcd for WC$_{22}$H$_{31}$N$_6$BO$_2$: C, 43.59; H, 5.15; N, 13.86. Found: C, 43.70; H, 5.13; N, 13.93.

Tp′(CO)$_2$W(η^3-CH$_2$CHCHPr^n) (4a,s). This complex was prepared by Method B with 1,5-hexadiene as the substrate and a photolysis time of 7 h. The orange product was obtained in 67% yield. Complex **4** was also synthesized by Method C through the thermal interconversion of the isomeric η^2-vinyl complex, Tp′(CO)$_2$W(η^2-C(Bu^n)=CH$_2$).[33] IR (KBr, cm^{-1}): ν_{BH} 2556; ν_{CO} 1917, 1819; ν_{CN} 1545. Anal. Calcd for WC$_{23}$H$_{33}$N$_6$BO$_2$: C, 44.54; H, 5.36; N, 13.55. Found: C, 44.66; H, 5.38; N, 13.64.

Tp′(CO)$_2$W(η^3-CH$_2$CHCHCH$_2$Ph) (5a,s). Method C: A sample of Tp′(CO)$_2$W(η^2-C(CH$_2$CH$_2$Ph)=CH$_2$)[33] was dissolved in toluene and allowed to reflux for 1 h. The solvent was removed, and the residue was chromatographed on alumina with CH$_2$Cl$_2$ as the eluent. Conversion to the η^3-allyl product was essentially quantitative. IR (KBr, cm^{-1}): ν_{BH} 2548; ν_{CO} 1910, 1815; ν_{CN} 1545. Anal. Calcd for WC$_{27}$H$_{33}$N$_6$BO$_2$: C, 48.53; H, 4.98; N, 12.58. Found: C, 48.41; H, 4.92; N,12.48.

Tp′(CO)$_2$W(η^3-CH$_2$CHCHPh) (6). Full characterization data for this compound as prepared through the hydride elaboration of a phenylacetylene complex has been given in the literature.[20,21] The present synthesis via a combination of Methods B and C with 3-phenyl propyne as the substrate produced a 34% yield. ^{13}C NMR (20 °C, CD$_2$Cl$_2$):[20,21] 230.3, 225.0 ($^1J_{WC}$ = 150, 180 Hz, *C*O), 140.5 (C_{ipso}), 128.0, 127.9, 126.3 (*Ph*), 81.5 (d, $^1J_{CH}$ = 170 Hz, η^3-CH$_a$H$_s$*C*H$_c$CH$_a$′Ph) 69.3 (d, $^1J_{CH}$ = 160 Hz, η^3-CH$_a$H$_s$CH$_c$*C*H$_a$′Ph), 50.5 (t, $^1J_{CH}$ = 158 Hz, η^3-*C*H$_a$H$_s$CH$_c$CH$_a$′Ph). ^{13}C NMR (−85 °C, CD$_2$Cl$_2$:CDCl$_3$:CCl$_4$, 60:27:13, δ): 229.6, 227.8 (*CO*), 139.2, 127.4, 126.8, 126.2 (*Ph*), 77.2, 76.1 (η^3-CH$_2$*CH*C*H*Ph), 59.8 ($^1J_{WC}$ = 22 Hz, η^3-*C*H$_2$-CHCHPh).

Tp′(CO)$_2$W(η^3-C(H)PhCHC(H)CH$_3$) (7a,s). Combination of Methods B and C: A solution containing 1.00 g (1.77 mmol) of Tp′(CO)$_3$WH and 0.50 mL (3.48 mmol) of 1-phenyl-1-butyne in 150 mL of THF was prepared. The IR spectrum after 6 h of irradiation showed an η^2-vinyl complex (1962 [1952], 1863 cm^{-1}) and the desired η^3-allyl complex (1917, 1829 cm^{-1}). The solvent was removed, and the oily residue was chromatographed on alumina with 6:1 hexanes:CH$_2$Cl$_2$ as the eluent. Broadening of the dark-colored band was evident, but no band separation was achieved. The solvent was removed to produce a brown solid. The solid was dissolved in 20 mL of toluene and allowed to reflux. The IR spectrum after 1 h indicated complete conversion to the allyl complex. The solvent was removed, and the residue was chromatographed on alumina with 1:1 heptane:CH$_2$Cl$_2$ as the eluent. Removal of the solvent yielded 0.470 g (40%) of a dark violet crystalline material. Full spectroscopic data is given in the Supporting Information. Essential NMR data is presented below; the notational scheme for complex **7** is given in Chart 4. IR (KBr, cm^{-1}): ν_{CO} 1902, 1808; ν_{CN} 1545; ^{1}H NMR (CDCl$_3$, δ): **7a** 4.92 (d,$^1J_{H_cH_a}$ = 10.4 Hz, *H$_a$*), 4.84 (qd, $^3J_{H_cH_s}$ = 8 Hz, $^3J_{MeH_s}$ = 6.4 Hz, *H$_s$*), 4.49 (dd, $^3J_{H_aH_c}$ = 10.4 Hz, $^3J_{H_sH_c}$ = 8 Hz, *H$_c$*), 1.78 (d, $^3J_{H_cH_a}$ = 6.4 Hz, *Me*); **7s** 5.42 (dd, $^3J_{H_{a(Me)}H_c}$ = 9.2, $^3J_{H_{a(Ph)}H_c}$ = 6 Hz, *H$_c$*), 3.24 (d,$^1J_{H_cH_{a(Ph)}}$ = 9.2 Hz, *H$_{a(Ph)}$*), 2.81 (qd, $^3J_{H_cH_s}$ = 6 Hz, $^3J_{MeH_{a(Ph)}}$ = 6 Hz, *H$_{a(Me)}$*), 2.46 (br, *Me*). ^{13}C NMR (C$_6$D$_6$, δ): **7a** 231.7 ($^1J_{WC}$ = 140 Hz, *C*O), 220.9 (*C*O), 92.0 (d, $^1J_{CH}$ = 164 Hz, *C*H$_c$), 74.7 (d, $^1J_{CH}$ = 163 Hz, *C*H$_a$), 58.6 (d, $^1J_{CH}$ = 153 Hz, *C*H$_s$), 17.7 (q, $^1J_{CH}$ = 125 Hz, *Me*); **7s** 228.2, 227.5 ($^1J_{WC}$ = 180, 160 Hz, *C*O), 79.9 (d, $^1J_{CH}$ = 169 Hz, *C*H$_c$), 72.8 (d, $^1J_{CH}$ = 157, *C*H$_{a(Ph)}$), 58.6 (d, $^1J_{CH}$ = 153 Hz, *C*H$_{a(Me)}$), 19.9 (q, $^1J_{CH}$ = 124 Hz, Me). Anal. Calcd for WC$_{27}$H$_{33}$N$_6$BO$_2$: C, 48.53; H, 4.98; N, 12.58. Found: C, 48.62; H, 4.95; N, 12.65.

Chart 4. Notational Scheme for Tp′(CO)$_2$W(η^3-C(H)PhCHC(H)CH$_3$), 7

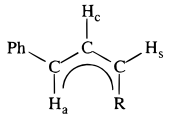

syn-phenyl-*anti*-methyl isomer (**6a**)

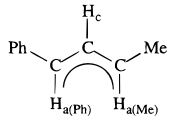

syn-phenyl-*syn*-methyl isomer (**6s**)

Table 6. Parameters Used in Extended Hückel Calculations

atom	orbital	H_{ii}, eV	ζ_1	ζ_2	C_1	C_2
W	5d	10.37	4.982	2.068	0.6940	0.5631
	6p	5.17	2.309			
	6s	8.26	2.341			
C	2p	11.40	1.625			
	2s	21.40	1.625			
O	2p	14.80	2.275			
	2s	32.30	2.275			
H	1s	13.60	1.300			

Table 7. Crystallographic Data Collection Parameters for η^3-Allyl Complexes

	2a	2b	7a	9	10a
mol form	$WC_{21}H_{29}N_6O_2B$	$WC_{21}H_{21}N_6O_2B$ (empirical)	$WC_{27}H_{33}N_6O_2B$	$WC_{20}H_{27}N_6O_2B$	$MoC_{21}H_{29}N_6O_2B$
fw, g/mol	592.15	584.9	668.25	490.22	
cryst dimens, mm	0.30 × 0.40 × 0.40	0.40 × 0.35 × 0.25	0.40 × 0.25 × 0.25	0.45 × 0.25 × 0.15	
space group	$P\bar{1}$	$P2_1/m$	$P\bar{1}$	$P\bar{1}$	$P\bar{1}$
cell params					
a, Å	10.248(2)	7.961(2)	9.634(5)	10.169(2)	10.280
b, Å	11.393(2)	13.176(2)	10.352(8)	11.090(2)	11.439(2)
c, Å	11.500(2)	11.192(4)	15.417(6)	11.369(2)	11.539(2)
α, deg	114.73(1)		98.21(4)	114.40(1)	114.71
β, deg	94.76(2)	103.84(3)	98.40(4)	98.84(1)	94.20
γ, deg	105.08(2)		117.47(5)	103.90(1)	104.95
vol, Å^3	3290.8(8)	1140.0(5)	1310.3(13)	1108.8(3)	
Z	2	2	2	2	
density calcd, g/cm^3	1.712	1.702	1.694	1.468	
radiation (wavelength, Å)	Mo Kα (0.710 73)	Mo Kα (0.710 73)	Mo Kα (0.710 73)	Mo Kα (0.710 73)	Mo Kα (0.710 73)
monochromator	graphite	graphite	graphite	graphite	graphite
linear abs coeff, cm^{-1}	51.6	52.0	45.4	60.0	
scan type	*θ*/2*θ*	*θ*/2*θ*	*θ*/2*θ*	*θ*/2*θ*	*θ*/2*θ*
2*θ* limit, deg	50.0	55.0	50.0	50.0	
quadrants collected	±*h*, +*k*, ±*l*	±*h*, +*k*, +*l*	±*h*, +*k*, ±*l*	±*h*, +*k*, ±*l*	±*h*, +*k*, ±*l*
total no. of reflns	4073	4394	5198	4316	
no. of data with $I \geq 2.5\sigma(I)$	3528	2299	4614	3381	
R, %	3.7	4.8	2.9	3.4	
R_w, %	4.6	5.7	4.1	5.2	
GOF	1.64	1.82	1.48	1.81	
no. of params	280	172	335	272	
largest param shift (shift/error ratio)	0.001	0.06	0.000	0.001	

Tp′(CO)$_2$W(η^3-C(H)CH$_3$CHC(H)CH$_2$CH$_3$) (8x,y). Method B: A solution containing 1.00 g (1.77 mmol) of Tp′(CO)$_3$WH and 0.22 mL (1.94 mmol) of 3-hexyne in 150 mL of THF was prepared. The solution was irradiated for 2.5 h. The IR spectrum at this time showed absorbances corresponding to the η^3-allyl product (1917, 1826 cm^{-1}) and a second species, presumably Tp′(CO)$_2$W(η^2-C(CH$_2$CH$_3$)═C(H)CH$_2$CH$_3$) (1930, 1848 cm^{-1}). After 19 h of stirring, the IR spectrum showed only the η^3-allyl product. The solvent was removed, and the residue was chromatographed on alumina with hexanes:CH$_2$Cl$_2$ (4:1) as the eluent. An orange-red band was collected. Solvent was removed to yield 0.560 g (51%) of an orange-red solid. IR (KBr, cm^{-1}): ν_{BH} 2554; ν_{CO} 1912, 1818; ν_{CN} 1546. ^{1}H NMR (−70 °C, CD$_2$Cl$_2$:CDCl$_3$:CCl$_4$, 60:27:13, *δ*): 5.86, 5.85, 5.83, 5.81, 5.80 (1:2:1:1:1, Tp′C*H* (both isomers)), 4.92 (dd, $^3J_{HH}$ = 9.2 Hz, $^3J_{HH}$ = 5. 2 Hz, H_c (1 isomer)), 4.86 (d (broad), $^3J_{HH}$ = 9.2 Hz, H_c (1 isomer)), 2.39, 2.35, 2.32, 2.30, 2.28, 2.03, 2.01 (9:6:3:12:3:3:3, Tp′C*H*$_3$ (both isomers), η^3-C(H)C*H*$_3$CHC(H)CH$_2$CH$_3$ (1 isomer)), 1.96 (dt, d-$^3J_{HH}$ = 5 Hz, t-$^3J_{HH}$ = 9 Hz, η^3-C(H)CH$_3$CHC(*H*)CH$_2$CH$_3$ (1 isomer)), 1.43 (m, η^3-C(H)CH$_3$CHC(H)C*H*$_2$CH$_3$ (1 isomer)), 1.32 (t, $^3J_{HH}$ = 7 Hz, η^3-C(H)CH$_3$CHC(H)CH$_2$C*H*$_3$ [1 isomer]), 0.80 (d, $^3J_{HH}$ = 6.1 Hz, η^3-C(H)C*H*$_3$CHC(H)CH$_2$CH$_3$ (1 isomer)), 0.61 (m, η^3-C(H)CH$_3$CHC(H)C*H*$_2$CH$_3$ (1 isomer)), 0.37 (t, $^3J_{HH}$ = 7.2 Hz, η^3-C(H)CH$_3$CHC(H)CH$_2$C*H*$_3$ (1 isomer)); the allyl protons on the methyl-substituted terminus for both isomers and the allyl proton on the ethyl-substituted terminus for one isomer could not be located unambiguously. ^{13}C NMR (−70 °C, CD$_2$Cl$_2$:CDCl$_3$:CCl$_4$, 60:27:13, *δ*)SPCLN 228.0, 227.9, 227.5, 227.0 (*C*O (both isomers)), 152.6, 151.8, 151.9, 149.8, 149.7, 145.3, 145.1, 144.1 (2:1:1:1:1:3:1:2, Tp′*C*CH$_3$ (both isomers)), 107.4, 107.1, 106.6 (2:2:2, Tp′*C*H (both isomers)), 85.0 (t, $^1J_{CH}$ = 173 Hz, η^3-C(H)CH$_3$*C*HC(H)CH$_2$CH$_3$ (1 isomer)), 83.6 (d, $^1J_{CH}$ = 171 Hz, η^3-C(H)CH$_3$*C*HC(H)CH$_2$CH$_3$ (1 isomer)), 80.1, 74.2, 64.2, 57.3 (d each, $^1J_{CH}$ = 150, 156, 150, 161 Hz, η^3-*C*(H)CH$_3$-CH*C*(H)CH$_2$CH$_3$ (both isomers)), 28.9, 22.5 (t each, $^1J_{CH}$ = 124, 125 Hz, η^3-C(H)CH$_3$CHC(H)*C*H$_2$CH$_3$ (both isomers)), 20.1, 20.0 (q each, $^1J_{CH}$ = 126, 126 Hz, η^3-C(H)CH$_3$CHC(H)CH$_2$*C*H$_3$ (both isomers)), 16.4, 16.1, 15.6, 14.9, 14.8, 13.2, 13.1, 13.0 (2:1:2:2:1:1:2, Tp′*C*H$_3$, η^3-C(H)*C*H$_3$CHC(H)CH$_2$CH$_3$ (both isomers)). Anal. Calcd for $WC_{23}H_{33}N_6BO_2$: C, 44.54; H, 5.36; N, 13.55. Found: C, 45.23; H, 5.56; N, 13.30 (Atlantic); C, 44.03; H, 6.01; N, 13.30 (Galbraith Laboratories, Inc., Knoxville, TN).

Tp′(CO)$_2$Mo(η^3-CH$_2$CHCH$_2$) (9). This complex was synthesized by Trofimenko's method.[1] IR (KBr, cm^{-1}): ν_{BH} 2544; ν_{CO} 1925, 1832; ν_{CN} 1545.

Tp′(CO)$_2$Mo(η^3-CH$_2$CHCHMe) (10a,s). This complex was prepared in a manner identical to that used by Joshi *et al.*[22] except that alumina rather than silica gel was used to purify the complex. Orange (82%). IR (KBr, cm^{-1}): **10a** ν_{BH} 2548; ν_{CO} 1919, 1827; ν_{CN} 1545; **10s** ν_{BH} 2546; ν_{CO} 1921, 1825; ν_{CN} 1545.

Extended Hückel Molecular Orbital (EHMO) Calculations. The extended Hückel program in the CAChe system (release 3.5) was used for this study. Parameters are given in Table 6. All W−C(O) bond distances were set at 1.95 Å, W−H at 1.70 Å, and C−O at 1.15 Å. All H−W−H and H−W−CO angles were set at 90°. The allyl fragment was located in a plane parallel to the *xy* plane and at a distance of 2.1 Å from the metal center. The bond angle of the allyl was fixed at 115°. The distances from the metal center to the terminal carbons were 2.409 Å, and the distance to the central allyl carbon was 2.231 Å. The allyl fragment was rotated about a point midway between the terminal carbons.

X-ray Diffraction Data Collection for the Tp′(CO)$_2$M(η^3-allyl) Complexes. Single crystals of the allyl complexes were mounted on glass wands coated with epoxy. Diffraction data were collected on a Rigaku diffractometer. Centered reflections found in the region 30.0° < 2*θ* < 40.0° were refined by least-squares calculations to indicate the unit cells. Unit cell and collection parameters for the allyl complexes are listed in Table 5. Diffraction data were collected in the appropriate hemispheres and under the conditions specified in Table 7. Only data with $I > 2.5\sigma(I)$ were used in structure solution and refinement[58] The data were corrected for Lorentz−polarization effects during the final stages of refinement.

Solution and Refinement of the *exo-Acute*-allyl Structures. The space group $P\bar{1}$ was confirmed for the *exo-acute*-allyl complexes and the positions of the metals were deduced from the three-dimensional Patterson functions. The positions of the remaining non-hydrogen atoms were determined through subsequent Fourier and difference Fourier calculations. All non-hydrogen atoms were refined anisotropically. Hydrogen

(58) Programs used during solution and refinement were from the NRCVAX structure determination package: Gabe, E. J.; Le Page, Y.; Charland, J. P.; Lee, F. L.; White, P. S. *J. Appl. Chem.* **1989**, *22*, 384.

atoms were calculated by using a C−H distance of 0.96 Å and an isotropic thermal parameter calculated from the anisotropic values for the atoms to which they were connected. The final residuals are indicated in Table 6.[59,60] The final difference Fourier maps had no peaks greater than 2.53, 1.63, and 0.600 e/Å^3 for **2a**, **7a**, and **9**, respectively.[61]

Solution and Refinement of the *meso-Obtuse*-allyl Structure. The space group $P2_1/m$ was confirmed, and the position of the tungsten was deduced from the three-dimensional Patterson function. The positions of the remaining non-hydrogen atoms were determined through subsequent Fourier and difference Fourier calculations. A crystallographic mirror plane containing one carbonyl group, the tungsten atom, one pyrazole group, the boron atom, and the allylmethyl group was found. Both the allyl moiety and the other carbonyl group were found to be disordered across the crystallographic mirror plane. The disorder was such that the carbon of the unsubstituted allyl terminus was coincident with the disordered carbonyl carbon. The 11 non-hydrogen atoms in the mirror plane and the 7 non-hydrogen atoms of the pyrazole group not contained in the mirror plane were refined anisotropically. The remaining carbonyl group and the allyl fragment were refined anisotropically, with reference to effective populations across the mirror plane. The final residuals[59] for 172 variables refined against 2299 data with $I > 2.5\sigma(I)$ were $R = 4.8\%$ and $R_w = 5.7\%$.[60] The final difference Fourier map had no peak greater than 4.31 e/Å^3.[61]

Acknowledgment. We thank the Department of Energy (Grant No. DE-FG02-96ER 14608), Division of Chemical Sciences, Office of Basic energy for generous support of this work. We also gratefully acknowledge Dr. S. G. Feng for his help at the outset of this work.

Supporting Information Available: Text giving full spectroscopic information for Tp′(CO)$_2$W(η^3-allyl) complexes not previously published, ORTEP representations showing complete numbering scheme, and tables of bond lengths and bond angles, atomic coordinates, and U_{ij} values (23 pages). Ordering information is given on any current masthead page.

OM970074S

(59) The function minimized was $\sum\omega(|F_o| - |F_c|)^2$, where ω is based on counter statistics.

(60) $R_{unweighted} = \sum(|F_o| - |F_c|)/\sum|F_o|)$, and $R_{weighted} = [\sum\omega(|F_o| - |F_c|)^2/\sum\omega F_o^2]^{1/2}$.

(61) Scattering factors were taken from the following: Cromer, D. T.; Waber, J. T. *International Tables for X-ray Crystallography*; Ibers, J. A., Hamilton, J. C., Eds.; Kynoch Press: Birmingham, England, 1974; Vol. IV, Table 2.2.

(62) **Note Added in Proof:** An alternative description of the variable-temperature NMR behavior of the closely related Tp′(CO)$_2$Mo(CH$_2$CHCHPh) was published while this paper was under review: Chowdhury, S. K.; Nandi, M.; Joshi, V. S.; Sarkar, A. *Organometallics* **1997**, *16*, 1806.